Efficient Evaluation of Process Stability in Milling with Spindle Speed Variation by using Chebyshev Collocation Method

Abstract

Chatter is a vibrational problem affecting machining operations, which may cause bad surface quality and damages to the machining system. In the last decades, several techniques for avoiding chatter onset were developed. Among other techniques, the continuous modulation of spindle speed during the cutting process (also called Spindle Speed Variation SSV) has been demonstrated to be very effective for avoiding chatter onset. However, spindle speed modulation parameters should be adequately optimized before machining, in order to allows one to achieve a real advantage when using this strategy for maximizing the material removal rate. In this perspective, chatter prediction algorithms play a crucial role, since they allow a preventive evaluation of process stability. State of the art algorithms for chatter prediction in milling with SSV are characterized by extremely long computation times, which are not acceptable for industrial applications. In this paper, an innovative and fast algorithm for chatter prediction in milling with SSV, based on the Chebyshev Collocation Method, is presented. The algorithm was successfully compared with a state of the art algorithm the Semi Discretization Method in different experimental configurations and cutting conditions. The results showed that the new method is generally more accurate and from ten to one thousand times faster than the Semi Discretization Method.

Keywords: Machining, Milling, Chatter, Prediction, Spindle Speed Variation

1. Introduction

Static deflections and relative dynamic vibrations between tool and workpiece during machining play a crucial role, since they may strongly affect dimensional accuracy and surface quality of the machined parts, hindering the achievement of some important manufacturing production targets.

Chatter is a vibrational problem affecting machining processes such as milling. It consists of anomalous dynamic vibrations which considerably deteriorate surface quality. Moreover, it may cause excessive tool wear rate and it may damage machine tool components. For these reasons, it should be absolutely avoided.

Chatter can be classified as primary or secondary. Primary chatter typically occurs at low spindle rotational speeds, and it is mainly due to the friction between the tool and the chip/workpiece on contact surfaces [1][2] or to other physical mechanisms [3].

However, the most common cause for chatter onset especially for medium and high spindle speeds is the secondary chatter, which is mainly due to the regenerative effect [4]. In milling, it is the influence of the undulation left on the workpiece by the previous tooth passage on the actual uncut chip thickness acting on the tooth passing through the same angular position.

Several strategies have been developed in the last decades for addressing this difficult problem. They can be roughly classified as:

- strategies based on *a priori* selection of an optimal, stable combination of cutting parameters by using chatter prediction methods [5][6];
- passive chatter suppression strategies, aiming at avoiding the phenomenon by including special mechanical components into the kinematic chain composed of machine tool, workpiece and tooling system, such as tool adaptors with high stiffness and damping [7], cutters with uneven teeth spacing [8] and other devices [9];
- semi-active chatter suppression strategies, aiming at disturbing chatter onset by continuously modulating the geometry of the cutting tool [10], the modal parameters of the tooling system [11] or kinematic parameters (for instance the spindle speed as in the Spindle Speed Variation approach);
- active chatter suppression techniques aiming at reducing tooling system

vibrations [12] or workpiece vibrations [13] by using feedback control loops involving sensors and actuators;

- other strategies based on fast chatter detection and automatic selection of new cutting parameters [14], or hybrid combinations of the afore mentioned approaches.

The idea of modulating spindle speed for enhancing the stability of the cutting process can be first attributed to the pioneering work of Stoferle et al. in 1972 [15]. In the following years this approach was further investigated, but most research works were focused on the turning process, as in the milestone work of Sexton and Stone [16]. Because of the considerably greater mathematical complexity necessary for describing milling operations with Spindle Speed Variation, first important contributions for understanding the milling case appeared only in the nineties, see for instance Tsao et al. [17].

Experimental results obtained in recent decades demonstrated that this approach does significantly enhance the stability of the cutting process, allowing greater material removal rates and thus a higher productivity. Nevertheless, SSV can be successfully implemented only with relatively light spindles, when the available spindle torque is quite high and when the fundamental frequency of the spindle speed modulation required by the machining operation is compatible with spindle drive dynamics [18].

However, a successful application of SSV does strongly rely on chatter prediction algorithms, which should be capable of preliminarily evaluating process stability for a given combination of cutting conditions and SSV parameters. Therefore, the development of accurate and computationally efficient methods for chatter prediction is crucial. In this paper, an innovative chatter prediction method for evaluating the stability of milling operations with SSV will be presented. Firstly, an overview of chatter prediction methods for machining operations with continuous spindle speed modulation will be illustrated. Afterwards, a dynamic model of milling will be introduced, as well as the criteria for stability evaluation and the innovative Chebyshev Collocation Method used for domain discretization. Eventually, a quantitative comparison between the proposed algorithm and the Semi Discretization Method will be carried out in terms of memory consumption and elaboration time, for a fixed level of accuracy of the parameter characterizing process stability.

2. Review on chatter prediction algorithms

Main result of chatter prediction algorithms are the stability lobes, which are obtained by evaluating process stability at different cutting parameter combinations (typically, different combinations of spindle speed and depth of cut), see Figure 1. It is worth noting that stability lobe minima are considerably increased when SSV is applied, in comparison to Constant Speed Machining. This vibration mitigation strategy allows to achieve a greater depth of cut without reducing any other cutting parameter hence assuring a greater material removal rate. Moreover, the position of the stability lobes with respect to spindle speed is greatly affected, and stability lobe borders become more jagged, when SSV is applied.

In order to perform process stability and to compute the stability lobes, different approaches were developed in recent decades. These approaches are generally quite complex since the milling process is modelled by a set of Delay Differential Equations DDEs with time periodic coefficients, as described in the next section. Unfortunately, no analytical closed form solution for the determination of the stability borders is available, unless some strong simplifications are assumed, which are detrimental for the prediction accuracy [5]. Accordingly, approximated numerical methods for studying process stability have to be applied. Basically, they can be classified as direct time domain integrations, frequency domain methods and DDEs-based methods, as illustrated in Table 1.

Direct time domain integration produces very reliable predictions since it takes into account complex phenomena such as the effective kinematics of milling, the loss of contact between active teeth and workpiece and many others [19][20], which are usually neglected by the linear analysis of stability. Unfortunately, this approach is in general very time consuming. In comparison to constant speed machining, even higher elaboration times are necessary for studying the SSV case, since integration has to be carried out on a longer time horizon in order to cope with the longer excitation period caused by spindle speed modulation [21][22]. Moreover, it is usually not easy to evaluate whether the system is stable or not, due to vibrational beatings which may arise in these conditions. For these reasons, direct numerical integration is not feasible for practical industrial applications.

Alternatively, frequency domain and DDEs-based methods are very promising, since they are capable of estimating process stability from system dynamic behavior without computing the time evolution of the system trajec-

Table 1: Overview of chatter prediction algorithms for stability evaluation of machining operations with continuous Spindle Speed Variation.

Process	Aim of the research	Analytical-numerical methods for stability evaluation	DoF adopted for numerical computations	Spindle Speed Modulation	Experimental validation	Ref.
Turning, boring	Effective on-line chatter suppression based on sinusoidal SSV technique	Analytical energy-based approach for the estimation of optimal parameters (amplitude and frequency) of sinusoidal spindle speed perturbation	1 DoF model	Sinusoidal with $RVA = 2 \div 30\%$; $RVF = 2 \div 20\%$	Carried out on horizontal CNC lathe by using coated carbide tools and 1018 carbon steel workpieces	[23]
Turning	Chatter suppression by applying SSV and/or time-varying (triangular) rake angle strategies	Numerical time varying spectrum method	1 DoF model	Sinusoidal with $RVA \leq 20\%$ and $RVF = 2 \div 6\%$	Carried out on a lathe by using a slender toolholder and by machining a stiff cylindrical 1040 carbon steel workpiece	[10]
Turning	New method for chatter prediction in turning with SSV. Optimization of SSV parameters	MFM: cutting process dynamics are analyzed in the frequency domain by considering the influence of SSV	1 DoF model	Sinusoidal with $RVA \leq 30\%$ and $RVF \leq 40\%$	Carried out on a lathe by using flexible toolholder with uncoated cutting insert and by machining a rigid 2024 aluminum workpiece. Other turning results found in literature are also considered	[24]
Milling	New method for chatter prediction in milling with SSV	Extension of the MFM to treat the more complicated case of milling	2 DoF model	Sinusoidal with $RVA \leq 30\%$ and $RVF \leq 50\%$	Face-milling tests with $D = 102$ mm cutter diameter and 8 teeth, on aluminum 2024 workpiece, in different configurations	[25]
Milling	Chatter prediction in milling with SSV. Comparison with SDM and simulation based on time integration. Optimization of SSV parameters	Refined MFM for modeling more general spindle speed perturbations with respect to previous works	1 Dof model	Sinusoidal with $RVA \leq 35\%$; $RVF \leq 35\%$. Numerical tests with triangular modulation	Carried out on milling machine by using $D = 80$ mm cutter diameter with $Z_t = 3$ teeth and by machining steel workpiece; half immersion down milling	[22]
Turning	Chatter suppression by SSV	Time discretization and Lyapunov Exponent as stability criterion	1 DoF model	Multi-level random perturbation with max. deviation = 25% and duration = 0.5 s; sinusoidal with $RVA < 25\%$ and $RVF < 12\%$	Carried out on horizontal CNC lathe by using coated carbide tools and 1018 carbon steel workpieces	[26]
Turning	Computationally efficient chatter prediction in turning with SSV	SDM; Direct Euler integration; Taylor expansion and Euler integration	1 DoF model	Sinusoidal with $RVA = 10\%$; $RVF = 20 \div 50\%$	Purely numerical	[21]
Turning	Application of SDM for studying the influence of SSV parameters on turning processes	SDM	1 DoF model	Sinusoidal with $RVA \leq 25\%$; $RVF \leq 40\%$	Numerical investigations and experimental case studies taken from literature	[27]
Milling	Studying the effect of SSV and of SSV parameters on system stability in the high spindle speed range	SDM	1 DoF model	Triangular with $RVA < 20\%$; $RVF < 1.3\%$	High speed milling tests with $D = 25$ mm cutter diameter and $Z_t = 3$ teeth on aluminum 2017A workpiece (characterized by high compliance in the transversal direction); down milling with 8% radial immersion	[28]
Milling	Studying the effect of SSV and of SSV parameters on system stability of up and down milling processes	SDM	1 DoF model	Sinusoidal with $RVA \leq 30\%$; $RVF \leq 30\%$	Purely numerical investigations on partial immersion up and down milling cases	[29]

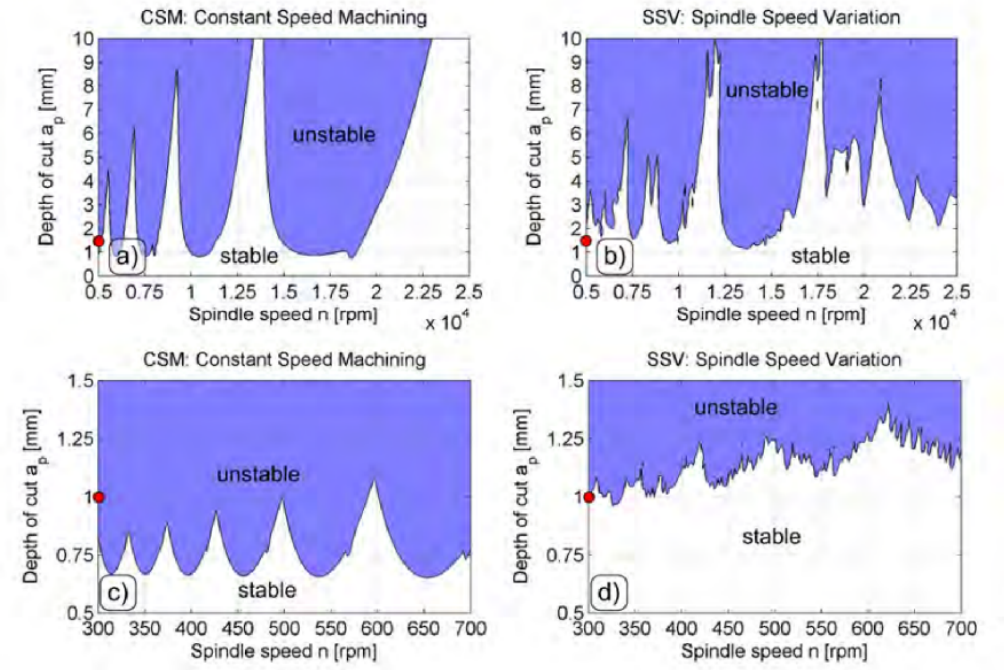

Figure 1: Examples of stability lobes obtained by considering different experimental configurations and spindle speed regimes. Specifically, figures above – a) and b) – refer to 10% down milling configuration with tool diameter $D = 12.7$, $Z_t = 2$ teeth and aluminum workpiece [31], while figures below – c) and d) – refer to a new experimental configuration introduced by the authors, i.e. 50% down milling configuration, with $D = 80$ mm, $Z_t = 6$ teeth and Ck45 workpiece. Stability diagrams obtained with Constant Speed Machining (CSM) – a) and c) – are compared to the stability diagrams obtained with sinusoidal Spindle Speed Variation (SSV) – b) and d) – with $RVA = 0.3$ and $RVF = 1/3$, see section 3. Stability lobes are computed by applying the new algorithm on a rectangular grid with 200 levels of spindle speed n and 100 levels of depth of cut a_p. Red points correspond to the cutting parameter combinations considered for the evaluation of the numerical convergence of the proposed algorithm, see section 6.

tory.

Frequency domain methods were first introduced by Altintas et al. in 1995 for studying the stability of conventional milling operations performed at constant spindle speed [30]. The concept of this method is to expand the

dynamic model of the system into a Fourier series and to assume that the perturbation of system vibrations with respect to forced vibrations be a periodic trajectory, which does neither extinguish nor diverge. Thus, for a given spindle speed n, the most conservative value of depth of cut $a_{p,cr}$ satisfying these assumptions is considered as the critical depth of cut corresponding to the stability borders.

In 2000, Jarayam et al. developed the Multi-Frequency Method (MFM) to analyze the turning process with SSV [24]. In this advanced approach, more harmonics were included in the calculations by taking into account the effects of spindle speed modulation for improving the accuracy of results. A couple of years later Sastry et al. [25] presented a Multi-Frequency Method for solving the milling process with SSV, although it was based on some strong simplifications which limited the applicability and accuracy of the method. A further refinement of the Multi-Frequency Method for studying the milling case was recently proposed by Zatarain et al. [22], who managed to treat more general spindle speed perturbations by overcoming most of the drawbacks affecting previous works. However, the achievement of the desired level of accuracy requires a careful calibration of several parameters, and the computations can be very time-consuming. Besides, this method is very complicated and difficult to reproduce because of poor implementation details found in the literature.

A radically different analytical perspective was adopted by the Semi Discretization Method (SDM) developed by Insperger et al. in 2004 [31] for constant speed milling: the stability analysis is accomplished by discretizing the original set of Delay Differential Equations in the time domain in order to assemble a special matrix called the monodromy matrix representing the dynamic transition of the system between one fundamental period and the following one. Afterwards, process stability is evaluated by computing the so called spectral radius, which is approximated by the maximum modulus of monodromy matrix eigenvalues. In general, the greater the number of time subintervals used for DDEs discretization, the more accurate is the estimate of spectral radius. However, a very large number of discretization subintervals may be required for achieving the desired accuracy, hindering the application of this method for practical purposes.

An extension of this method for studying the milling process with SSV was recently developed by Seguy et al. [28], who approximated the modulated time delay between subsequent teeth by means of stepwise constant trends. The approach is very promising, nevertheless its numerical convergence to

the theoretical solution was not adequately investigated.

According to the qualitative comparison carried out by Zatarain et al. [22], there is in general a good agreement between the stability lobes predicted by MFM and those predicted by SDM. However, some important discrepancies were also detected, which were likely to be due to convergence issues not discussed by the authors.

The only semi-quantitative comparison between the two methods can be found in [5] for constant speed milling operations, where the authors reported that MFM was approximately two times faster than SDM.

A novel approach for achieving a considerably faster convergence of the approximated solution of DDEs to the theoretical one is the Chebyshev Collocation Method described by Bueler in 2004 [32] and applied in milling by Butcher et al. in 2005 [33].

A numerical comparison between this approach and SDM was presented by Kuljanic et al.[34] by analyzing different milling operations performed at constant spindle speed. For a given level of accuracy, the Chebyshev Collocation Method proved to be from ten to one thousand times faster than SDM.

Although the mathematics underlying both MFM and SDM can be applied to 2DoF models, it is worth noting that they were almost exclusively tested on 1DoF numerical examples, as evidenced in Table 1.

In this paper, a 2DoF dynamic model of the cutting process based on Delay Differential Equations expressed in the angle domain, together with an innovative extension of the DDE stability criteria and of the Chebyshev Collocation Method for efficient analysis of milling operations with Spindle Speed Variation is presented. Finally, the numerical performance of the new method is successfully compared to that of SDM.

3. Milling Dynamics

Chatter prediction methods are based on the joint analysis of machining system dynamics, cutting forces and cutter-workpiece dynamic interaction.

3.1. Machining system dynamics

The spindle - spindle adaptor -tooling system is modeled as a Jeffcott rotor [35] rotating at constant speed n around its main axis and vibrating along the two directions orthogonal to cutter axis of an inertial, non rotating coordinate frame, see Figure 2. Also, the system is usually considered rigid

in the axial and torsional directions. Accordingly, only transverse tool tip vibrations in the working plane OXY are relevant, and are described by

$$\underbrace{\begin{bmatrix} u_x(j\omega) \\ u_y(j\omega) \end{bmatrix}}_{\mathbf{u}(j\omega)} = \underbrace{\begin{bmatrix} W_{xx}(j\omega) & W_{xy}(j\omega) \\ W_{yx}(j\omega) & W_{yy}(j\omega) \end{bmatrix}}_{\mathbf{W}(j\omega)} \underbrace{\begin{bmatrix} F_x(j\omega) \\ F_y(j\omega) \end{bmatrix}}_{\mathbf{F}(j\omega)} \tag{1}$$

where W_{ii} are the direct transfer functions and W_{ij} are the cross transfer functions. In most cases of practical interest, cross transfer functions are negligible while direct transfer functions are both approximated by a single mass-spring-damper system [36][37]. However, direct transfer functions are in general composed of several modes of vibrations [38], which can be modeled as follows

$$W_{ii}(j\omega) = \frac{u_i(j\omega)}{F_i(j\omega)} = \sum_{k=1}^{M_i} \frac{G_{i,k}}{(j\omega/\omega_{ni,k})^2 + 2\xi_{i,k}(j\omega/\omega_{ni,k}) + 1}, \quad i = x, y \tag{2}$$

where $G_{i,k}$ is the zero frequency gain, $\omega_{ni,k}$ is the natural pulsation and $\xi_{i,k}$ is the damping coefficient of the k_{th} mode of vibration acting along direction i. For the sake of simplicity, the workpiece is considered to be rigid.

3.2. Cutting force model

Cutting forces depend on several factors, such as cutting parameters, workpiece material, cutter geometry and milling process geometry. Let us consider a cutter with Z_t equally-spaced cutting inserts and with generic cutting edge lead angle χ. Let the nose radius r_ε be negligible in comparison to the depth of cut a_p. Under this hypothesis, local cutting edge geometry is approximately constant along the engaged cutting edge. In order to model the cutting forces it is necessary to recall the instantaneous chip thickness acting on the j^{th} tooth $h_j(t)$ and the length of the engaged (main) cutting edge

$$b = \frac{a_p}{\sin\chi} \tag{3}$$

where ξ is the working cutting edge angle. The shearing and ploughing cutting force model can be adopted for the main cutting force $F_{c,j}$ and for the perpendicular cutting force $F_{cN,j}$ acting on the j^{th} tooth, as follows

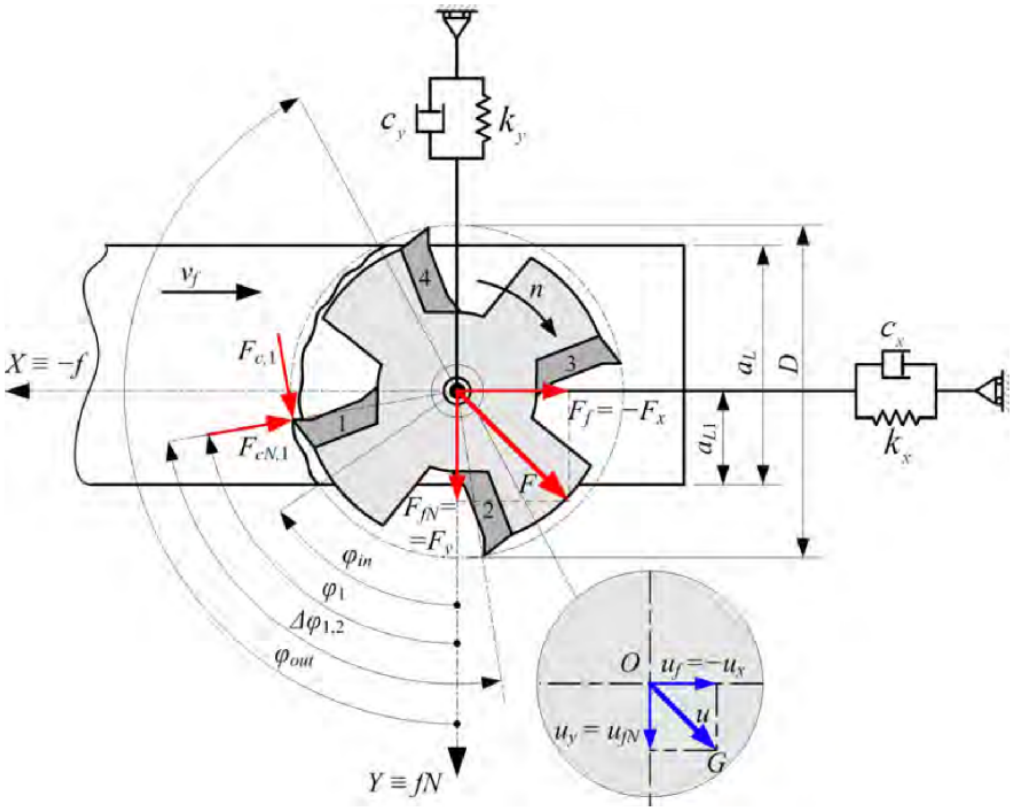

Figure 2: Reference scheme for relative tool-workpiece vibrations

$$\begin{cases} F_{c,j}(t) \cong k_{cs} h_j(t)\, b + k_{cp} b \\ F_{cN,j}(t) \cong k_{cNs} h_j(t)\, b + k_{cNp} b \end{cases} \tag{4}$$

where k_{ws} $(w = c, cN)$ are the shearing coefficients modelling the effect of chip pressure on the normal rake face while k_{wp} $(w = c, cN)$ are the ploughing coefficients modelling the friction between the machined surface and the main cutting edge, respectively [38][39].

3.3. Cutter-workpiece dynamic interaction

Let Ω be the angular spindle speed expressed in rad/s. Under constant spindle speed conditions,

$$\Omega = \frac{2\pi n}{60} = \frac{2\pi}{T} \tag{5}$$

n being the (constant) spindle speed expressed in rpm and T the (constant) spindle revolution period. Let us introduce the time delay between subsequent teeth τ. Under the hypothesis of constant speed machining and an equally spaced teeth cutter, the time delay τ is given by

$$\tau = \frac{T}{Z_t} = \frac{60}{nZ_t} \tag{6}$$

where Z_t is the teeth number.

Let us now introduce the angular pitch (angular delay) $\Delta\varphi_z$ between subsequent teeth, which is always (both with constant and variable speed machining) given by

$$\Delta\varphi_z = \frac{2\pi}{Z_t} \tag{7}$$

provided that the teeth are equally spaced.

Let us consider the feed motion angle of the first tooth $\varphi_{z,1}$ for representing the angular position of the whole cutter

$$\varphi = \varphi_{z1} \tag{8}$$

Then, the feed motion $\varphi_{z,j}$ of the j^{th} tooth can be expressed by

$$\varphi_{z,j} = \varphi - (j-1)\,\Delta\varphi_z, \qquad j = 1, \ldots, Z_t \tag{9}$$

Under general SSV conditions we have a generic spindle speed behavior $\Omega(t)$ which is assumed to be $T'_\Omega-$periodic.

As assumed by several authors [21][27][28], the ratio of the effective spindle speed modulation period T'_Ω to the nominal time delay τ or to the nominal spindle revolution period T can be approximated by a rational number with sufficient accuracy, as follows

$$\left.\begin{array}{l}\text{No teeth runout}: \ T'_\Omega/\tau \\ \text{With teeth runout}: T'_\Omega/T\end{array}\right\} \cong \frac{L}{P} \qquad \text{with } P, L \in \mathbb{N} \tag{10}$$

Thus, it is possible to find an integer multiple T_Ω of the effective spindle modulation period T'_Ω which is concurrently an integer multiple of the nominal time delay τ or of the nominal spindle revolution period T, i.e.

$$T_\Omega = PT'_\Omega \cong \left\{\begin{array}{ll} L\tau & (\text{no teeth runout}) \\ LT & (\text{with teeth runout})\end{array}\right. , \qquad \text{with } P, L \in \mathbb{N} \tag{11}$$

Accordingly, when expressed in the angular domain the function $\Omega(\varphi)$ is $\Delta\varphi_\Omega$-periodic, where the angular period $\Delta\varphi_\Omega$ can be thought as a multiple of the fundamental angular period $\Delta\varphi_z$ or of one revolution period 2π by means of the same integer L, that is

$$\Delta\varphi_\Omega \cong \begin{cases} L\Delta\varphi_z & (\text{no teeth runout}) \\ L2\pi & (\text{with teeth runout}) \end{cases} \tag{12}$$

Only feasible spindle speed modulations are considered here. Accordingly, spindle speed modulation is assumed to be continuous and with piecewise continuous first derivative (i.e. stepwise $\mathcal{C}^1$), and such that the resulting spindle speed is always positive, i.e.

$$\Omega(t) = \frac{d\varphi}{dt}(t) > 0 \quad \forall t \tag{13}$$

which is essential for the time to angle transformation described in the following.

When sinusoidal spindle speed modulation is considered, as in section 6, it can be expressed in the following form

$$\Omega(t) = \Omega_0 + RVA \cdot \Omega_0 \cos(RVF \cdot \Omega_0 t) \tag{14}$$

where Ω_0 is the nominal, average spindle speed, RVA is the amplitude modulation coefficient and RVF is the frequency modulation coefficient. In most practical cases of interest, both coefficients range in the interval [0,0.3].

Anyway, it must be pointed out that the proposed algorithm is capable of treating other types of spindle speed modulations (such as triangular-like and random-like), without requiring any further simplification.

The instantaneous feed motion angle of the cutter is given by

$$\varphi(t) \equiv \varphi_{z1}(t) = \varphi(t_0) + \int_{t_0}^{t} \Omega(\sigma)\, d\sigma \tag{15}$$

which is continuous, with continuous first derivative, and stepwise $\mathcal{C}^1$. Besides, it is monotonically increasing thanks to Equation (13) and thus invertible, i.e. the function

$$t = t(\varphi) \tag{16}$$

is well defined: it represents the time evolution with respect to the reference feed motion angle φ. In order to model the engagement of each tooth in the

workpiece, the window function g_j is introduced, as follows

$$g_j = g_j(\varphi) = g(\varphi_{zj}) = \begin{cases} 1 & \text{if } \varphi_{in} < \varphi_{zj} < \varphi_{out} \\ 0 & \text{elsewhere} \end{cases} \tag{17}$$

being φ_{in} and φ_{out} the entrance and exit angles, respectively, recalling that $\varphi_{zj} \in [0, 2\pi]$ is the feed motion angle of the j^{th} tooth given by Equation (9).

Let us further define

$$\begin{cases} s_j(\varphi) = \sin(\varphi_{zj}) = \sin(\varphi - (j-1)\Delta\varphi_z) \\ c_j(\varphi) = \cos(\varphi_{zj}) = \cos(\varphi - (j-1)\Delta\varphi_z) \end{cases} \tag{18}$$

In general, the theoretical instantaneous chip thickness h_{j0} acting on the j^{th} tooth can be approximated by

$$h_{j0}(\varphi) \cong g_j(\varphi) f_{zj}(\varphi) \mathrm{s}_j(\varphi) \sin\chi \tag{19}$$

where

$$f_{zj}(\varphi) = \frac{v_f}{60}\tau(\varphi) + \delta_j \tag{20}$$

being τ the time delay between subsequent teeth, v_f the linear feed speed expressed in mm/min, and δ_j the radial runout expressed in mm given by the difference

$$\delta_j = r_j - r_{j-1} \tag{21}$$

where r_j is the radius of the j^{th} tooth. It should be recalled that

$$\sum_{1}^{z_t} \delta_j = 0 \tag{22}$$

When spindle speed is constant, the time delay is given by Equation (6). On the contrary, when SSV is applied, the modulated time delay can be derived from Equation (16), as follows

$$\tau(\varphi) = t(\varphi) - t(\varphi - \Delta\varphi_z) \tag{23}$$

which is a piecewise $\mathcal{C}^2$, $\Delta\varphi_\Omega$-periodic function of the feed motion angle.

Hence, for a general SSV application the period of the "static" instantaneous chip thickness $h_{j0}(\varphi)$ is $\Delta\varphi_\Omega$ instead of 2π.

By also considering tool tip vibrations, one should add

$$h_j(\varphi) \cong \underbrace{h_{j0}(\varphi)}_{\Delta\varphi_\Omega-\text{periodic}} + \underbrace{[g_j(\varphi)\, s_j(\varphi)]}_{2\pi-\text{periodic}} \underbrace{[u_x(\varphi) - u_x(\varphi-\Delta\varphi_z)]}_{\text{regenerative perturbation}} + \\ + \underbrace{[g_j(\varphi)\, c_j(\varphi)]}_{2\pi-\text{periodic}} \underbrace{[u_y(\varphi) - u_y(\varphi-\Delta\varphi_z)]}_{\text{regenerative perturbation}} = \underbrace{h_{j0}(\varphi)}_{\Delta\varphi_\Omega-\text{periodic}} + \underbrace{h_{j\delta}(\varphi)}_{\text{perturbation}} \tag{24}$$

where $h_{j\delta}$ is the perturbation due to the interference between the current vibration ($u(\varphi)$) and on the undulation left on the machined surface by the previous tooth passage ($u(\varphi-\Delta\varphi_z)$), namely the regenerative effect.

The linearization of cutting forces with respect to the "static", periodic chip thickness h_{j0} yields

$$F_{w,j}(\varphi) \cong F_{w,j}(h_{j0}(\varphi)) + \frac{\partial F_{w,j}}{\partial h_j}(h_{j0}(\varphi))\, h_{j\delta}(\varphi) = \underbrace{F_{w,j0}(\varphi)}_{\Delta\varphi_\Omega-\text{periodic}} + \underbrace{F_{w,j\delta}(\varphi)}_{\text{perturbation}}, \\ w = c, cN \tag{25}$$

where the first term is due to the nominal chip thickness, while the force perturbation derives from the regenerative effect. The resultant cutting force can be obtained by adding the contributions $F_{w,j}$ projected along the X and Y axes, taking into account the instantaneous feed motion angles φ_{zj}, as follows,

$$\begin{cases} F_x(\varphi) = \sum_{j=1}^{Z_t} \left(-F_{c,j}(\varphi)\, c_j(\varphi) - F_{cN,j}(\varphi)\, s_j(\varphi)\right) \\ F_y(\varphi) = \sum_{j=1}^{Z_t} \left(F_{c,j}(\varphi)\, s_j(\varphi) - F_{cN,j}(\varphi)\, c_j(\varphi)\right) \end{cases} \tag{26}$$

Accordingly, it is possible to decompose the resultant into

$$\begin{bmatrix} F_x(\varphi) \\ F_y(\varphi) \end{bmatrix} = \mathbf{F}(\varphi) \cong \mathbf{F}_0(\varphi) + \mathbf{F}_\delta(\varphi) = \\ = \underbrace{\mathbf{F}_0(\varphi)}_{\substack{\Delta\varphi_\Omega-\text{periodic} \\ \text{vector}}} + \underbrace{\mathbf{F'}_1(\varphi)}_{\substack{\Delta\varphi_z \text{ or } 2\pi- \\ \text{periodicmatrix}}} (\mathbf{u}(\varphi) - \mathbf{u}(\varphi-\Delta\varphi_z)) \tag{27}$$

where $\mathbf{F_0}$ is the "static" contribution due to the nominal chip thickness and $\mathbf{F_\delta}$ is the "dynamic" term due to the regenerative effect. The matrix $\mathbf{F'_1}$ is $\Delta\varphi_z$ or 2πperiodic, depending on whether teeth radial run-out is negligible or not, respectively. In both cases, it has to be recalled that the angular period $\Delta\varphi_\Omega$ is an integer multiple of such a period.

Accordingly, both terms $\mathbf{F_0}$ and $\mathbf{F'_1}$ can be considered $\Delta\varphi_\Omega$periodic. An example of "static" cutting force trends in the time and frequency domains obtained with constant speed and with spindle speed modulation is shown in Figure 3. In comparison with CSM, SSV causes a general redistribution of spectral energy between a larger number of harmonics, tending towards a white noise behavior, reducing the probability of exciting system mechanical resonances by means of very high spectral peaks of the nominal cutting forces.

Let us consider a state space form (in the time domain) equivalent to Equation (1), i.e.

$$\begin{cases} \frac{d\mathbf{q}}{dt}(t) = \mathbf{A_W q}(t) + \mathrm{B_W F}(t) \\ \mathbf{u}(t) = \mathbf{C_W q}(t) \end{cases} \tag{28}$$

where $\mathbf{q}$ is the state vector (with d state variables), $\mathrm{A_W}$, $\mathrm{B_W}$, $\mathrm{C_W}$ are the state space matrices representing a time realization of the transfer function $\mathbf{W}(\mathrm{j}\omega)$, $\mathbf{F}$ is the input (force) vector and $\mathbf{u}$ is the output (displacement) vector of the tool tip at time t. Time realization is chosen such that tool tip vibrations along X and Y directions can be directly derived from the first two state space variables, that is

$$\begin{cases} u_x = q_1 \\ u_y = q_2 \end{cases} \tag{29}$$

This is achieved when the output matrix of the adopted time realization is

$$\mathbf{C_W} = \begin{bmatrix} 1 & 0 & 0 & \cdots & 0 \\ 0 & 1 & 0 & \cdots & 0 \end{bmatrix} \tag{30}$$

This choice is particularly important in order to allow monodromy matrix size reduction before eigenvalue computation.

Let us now focus on the independent variable substitution

$$t \rightarrow \varphi \tag{31}$$

by using the well-defined function $t(\varphi)$ of Equation (16).

After substitution of (27) into the system (28), the following system of Delay Differential equations - DDEs can be obtained

$$\begin{cases} \frac{d\mathbf{q}}{dt}(\varphi) = \underbrace{\left(\mathbf{A_W} + \mathbf{B_W F'}_1(\varphi)\,\mathbf{C_W}\right)}_{\mathbf{A_{W1}}}\mathbf{q}(\varphi) + \underbrace{\left(-\mathbf{B_W F'}_1(\varphi)\,\mathbf{C_W}\right)}_{\mathbf{B_{W1}}}\mathbf{q}(\varphi - \Delta\varphi_z) + \\ \qquad + \underbrace{\mathbf{B_W F_0}(\varphi)}_{\mathbf{B_{W0}}} \\ \mathbf{u}(\varphi) = \mathbf{C_W q}(\varphi) \end{cases} \tag{32}$$

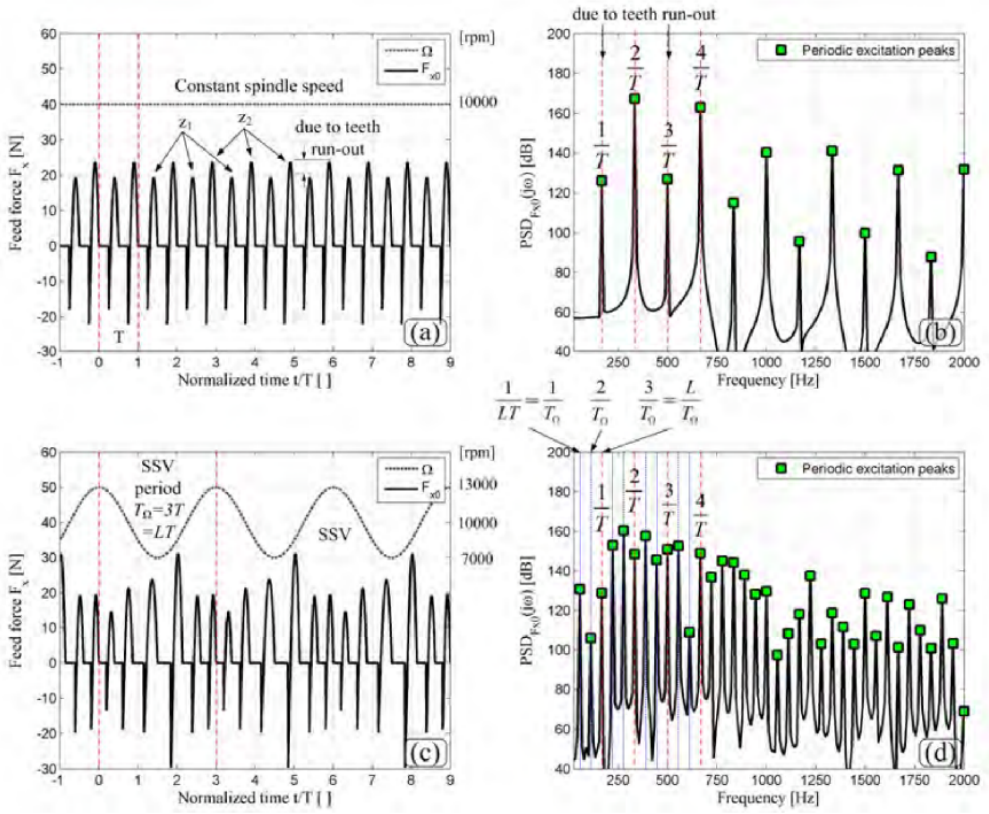

Figure 3: Behavior of "static" feed force in the time and frequency domains during constant speed machining ((a) and (b)) and when SSV is applied ((c) and (d)). End-mill cutter with $D = 12.7$ mm, $Z_t = 2$ teeth; down milling with radial immersion $a_L/D = 50\%$; spindle speed $\Omega = 10000$ rpm, depth of cut $a_p = 1$ mm, nominal feed per tooth $f_z = 0.1$ mm, radial runout $\delta_i = [0.01, -0.01]$ mm; cutting force coefficients $k_{cs} = 600$ MPa, $k_{ns} = 200$ MPa, $k_{cp} = k_{np} = 0$. SSV parameters: $RVA = 0.3$, $RVF = 1/3$.

Let us now express the derivative with respect to time in the following form

$$\frac{d\mathbf{q}}{dt} = \frac{d\mathbf{q}}{d\varphi}\frac{d\varphi}{dt} \tag{33}$$

similarly to the method originally proposed by Tsao et al. in 1993 [17], who applied this transformation for studying machining processes when SSV is in-

volved. However, they only applied this approach to single degree of freedom models, which were not adequate for describing the complex dynamics of milling processes. Later this transformation was also adopted by Pakdemirli et al. [40] and by Yang et al. [10], but their analysis was again limited to single degree of freedom models, which gave satisfactory results only in the simple case of turning.

Let us define the function

$$\psi(\varphi) = \frac{1}{\frac{d\varphi}{dt}(t(\varphi))} \tag{34}$$

which is the reciprocal of the instantaneous spindle speed expressed with respect to the reference feed motion angle φ.

Then the system (32) can be rewritten as

$$\begin{cases} \frac{d\mathbf{q}}{d\varphi}(\varphi) = \underbrace{\psi(\varphi)\mathbf{A_{W1}}(\varphi)}_{\mathbf{A}(\varphi)}\mathbf{q}(\varphi) + \underbrace{\psi(\varphi)\mathbf{B_{W1}}(\varphi)}_{\mathbf{B}(\varphi)}\mathbf{q}(\varphi - \Delta\varphi_z) + \\ \quad + \underbrace{\psi(\varphi)\mathbf{B_{W0}}(\varphi)}_{\mathbf{B}_0(\varphi)} \\ \mathbf{u}(\varphi) = \mathbf{C_W}\mathbf{q}(\varphi) \end{cases} \tag{35}$$

where $\mathbf{A}$ and $\mathbf{A}$ are $\Delta\varphi_\Omega$-periodic dxd matrices and $\mathbf{B}_0$ is a $\Delta\varphi_\Omega$-periodic $dx1$ column vector, where the period $\Delta\varphi_\Omega$ is an integer multiple of the fundamental delay $\Delta\varphi_z$. Under the above assumptions, such matrices and vectors are piecewise $\mathcal{C}^1$.

It is important to notice that the original time delay $\tau(t)$ was timevarying because of the continuous spindle speed modulation. On the contrary, a new set of DDEs with fixed delay $\Delta\varphi_z$ was obtained thanks to the time to angle domain transformation. This result allows one to avoid the approximation of the delayed term introduced by Seguy et al. [28] for adapting the Semi Discretization Method to milling operations with SSV, as illustrated in section 6. However, the most important consequence of this transformation was the possibility of a direct application of the Chebyshev Collocation Method for studying milling operations perturbed by general spindle speed modulations.

Accordingly, for the sake of comparison both the Semi Discretization Method and the Chebyshev Collocation Method will be applied on the same dynamic model (35) expressed in the angle coordinate.

The total vibration $\mathbf{q}(\varphi)$ is generally interpreted as the sum of "static" forced vibrations due to $\mathbf{B}_0(\varphi)$ and "dynamic" regenerative vibrations arising from the difference $(\mathbf{q}(\varphi) - \mathbf{q}(\varphi - \Delta\varphi_z))$. In the simple case of constant

speed machining, these terms can be studied separately by applying the superposition principle. Here on the contrary this commonly adopted approach is not feasible, since the period $\Delta\varphi_\Omega$ is different from the fundamental period $\Delta\varphi_z$. As a consequence, forced vibrations cannot be decoupled from the regenerative vibrations, and the stability criteria have to be based on the analysis of the system (35) taken as a whole.

4. Criteria for process stability evaluation

The general criteria for assessing the stability of a set of Delay Differential Equations can be found in [32]. In this section, an innovative extension of such criteria to Delay Differential Equations modelling complex milling processes with SSV - including both the forced and regenerative terms - is presented. In order to evaluate whether the system (35) is stable or not, let us split the fundamental period of the spindle speed perturbation $[0, \Delta\varphi_\Omega]$ into L intervals of equal span $\Delta\varphi_z$ (or 2π in case of significant teeth runout, see Equation (12)), as illustrated in Figure 4a), whose endpoints are located at

$$\varphi_l = l\Delta\varphi_z, \quad l = 0, 1, ..., L \tag{36}$$

where the l^{th} interval endpoint φ_l has not to be confused with φ_{zj}, which is the instantaneous feed motion angle of the j^{th} tooth.

Let us further define

$$S_{(l)} = [\varphi_{l-1}, \ \varphi_l], \quad l = 1, ..., L \tag{37}$$

as the l^{th} angle interval. From now on, subscripts enclosed between round brackets will be used to denote quantities defined over intervals rather than at single points.

Let us consider the linear, autonomous equation

$$\begin{cases} \frac{d\mathbf{q}}{d\varphi}(\varphi) = \mathbf{A}(\varphi)\,\mathbf{q}(\varphi), & \varphi \in S_{(l+1)} \\ \mathbf{q}(\varphi_l) = \mathbf{q}_{0l} \end{cases} \tag{38}$$

Since $\mathbf{A}(\varphi)$ is piecewise $\mathcal{C}^1$, the fundamental solution exists such that

$$\begin{cases} \frac{d}{d\varphi}\mathbf{\Phi_A} = \mathbf{A}(\varphi)\,\mathbf{\Phi_A}(\varphi), & \varphi \in S_{(l+1)} \\ \mathbf{\Phi_A}(\varphi_l) = \mathbf{I} \end{cases} \tag{39}$$

where $\mathbf{\Phi_A}$ is an invertible dxd matrix of functions and $\mathbf{I}$ is the identity dxd matrix [41].

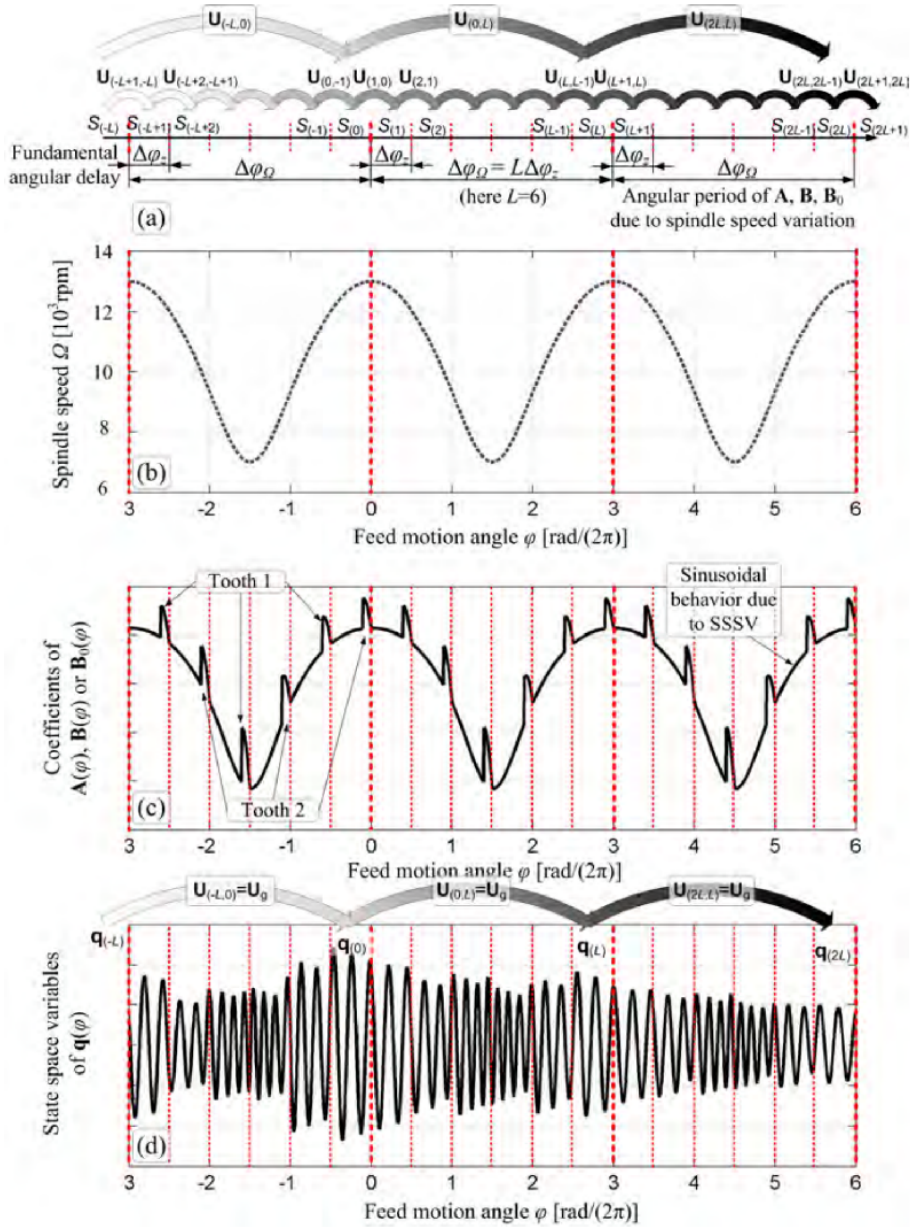

Figure 4: (a) Decomposition of angular domain into subintervals and monodromy operators; (b) sinusoidal spindle speed variation; (c) periodic matrix coefficients; (d) state space variables behavior. End-mill cutter with $D = 12.7$ mm, $Z_t = 2$ teeth; down milling with radial immersion $a_L/D = 10\%$; nominal spindle speed $\Omega = 10000$ rpm, depth of cut $a_p = 1$ mm, nominal feed per tooth $f_z = 0.1$ mm, radial runout $\delta_i = [0.01, -0.01]$ mm; cutting force coefficients $k_{cs} = 600$ MPa, $k_{ns} = 200$ MPa, $k_{cp} = k_{np} = 0$; modal parameters: see Table 3, [31]. SSV parameters: $RVA = 0.3$, $RVF = 1/3$.

In order to study the dynamic evolution of the solution $\mathbf{q}$, when the angle (i.e., the time) tends to infinity, let us suppose that we know its behaviour in the l^{th} angular interval $S_{(l)}$ and we want to determine its behaviour in the next subinterval $S_{(l+1)}$. Thus we may write

$$\begin{aligned}\mathbf{q}(\varphi) = &\left[\mathbf{\Phi_A}(\varphi)\,\mathbf{q}(\varphi_l) + \mathbf{\Phi_A}(\varphi)\int_{\varphi_l}^{\varphi}\left(\mathbf{\Phi_A}(\vartheta)\right)^{-1}\mathbf{B}(\vartheta)\,\mathbf{q}(\vartheta-\Delta\varphi_z)\,d\vartheta\right] + \\ &+\left[\mathbf{\Phi_A}(\varphi)\int_{\varphi_l}^{\varphi}\left(\mathbf{\Phi_A}(\vartheta)\right)^{-1}\mathbf{B}_0(\vartheta)\,d\vartheta\right]; \quad \varphi\in S_{(l+1)}=[\varphi_l,\varphi_{l+1}]\end{aligned} \tag{40}$$

In order to simplify notation, let us denote the state space trajectory in the $(l+1)^{th}$ interval as

$$\mathbf{q}_{(l+1)} \equiv \mathbf{q}(\varphi): \quad S_{(l+1)} \to \mathbb{R}^d \tag{41}$$

Accordingly, the delayed state space trajectory $\mathbf{q}(\varphi-\Delta\varphi_z)$, $\varphi\in S_{(l+1)}$ corresponds to $\mathbf{q}_{(l)}\equiv\mathbf{q}(\varphi)$, $\varphi\in S_{(l)}$.

Let us denote the linear operator transforming the state space trajectory $\mathbf{q}_{(l)}$ into the first term within square brackets on the right of Equation (40) as

$$\mathbf{U}_{(l+1,l)}:\boldsymbol{\mathcal{C}}\left(S_{(l)}\right)\longrightarrow\boldsymbol{\mathcal{C}}\left(S_{(l+1)}\right) \tag{42}$$

where $\boldsymbol{\mathcal{C}}(S)$ is the space of $\mathbb{R}^d$-valued continuous functions defined on the interval S.

The second term within square brackets on the right of Equation (40) will be simply denoted by $\mathbf{w}_{(l+1)}$. Therefore, Equation (40) can be rewritten in more compact form as

$$\mathbf{q}_{(l+1)} = \mathbf{U}_{(l+1,l)}\mathbf{q}_{(l)} + \mathbf{w}_{(l+1)} \tag{43}$$

In Figure 4, an example of system trajectory $\mathbf{q}$ including both static and dynamic effects is shown. Sinusoidal spindle speed modulation illustrated in Figure 4b) is responsible for the periodic behaviour of matrix coefficients shown in Figure 4c). Besides, spindle modulation causes the continuous modulation of system natural frequencies, when system vibrations are represented in the angular domain, see Figure 4d).

Let us now iteratively construct the whole solution in the spindle speed modulation period $[0,\Delta\varphi_\Omega]=[\varphi_0,\varphi_L]$, starting from its (known) history $\mathbf{q}_{(0)}\equiv\mathbf{q}(\varphi)$, with $\varphi\in S_{(0)}=[\varphi_{-1},\varphi_0]$:

$$\mathbf{q}_{(1)} = \mathbf{U}_{(1,0)}\mathbf{q}_{(0)} + \mathbf{w}_{(1)} \tag{44}$$

In the following interval $S_{(2)}$ we obtain

$$\begin{aligned}\mathbf{q}_{(2)} &= \mathbf{U}_{(2,1)}\mathbf{q}_{(1)} + \mathbf{w}_{(2)} = \mathbf{U}_{(2,1)}\left(\mathbf{U}_{(1,0)}\mathbf{q}_{(0)} + \mathbf{w}_{(1)}\right) + \mathbf{w}_{(2)} = \\ &= \mathbf{U}_{(2,1)}\mathbf{U}_{(1,0)}\mathbf{q}_{(0)} + \mathbf{U}_{(2,1)}\mathbf{w}_{(1)} + \mathbf{w}_{(2)}\end{aligned} \tag{45}$$

At the L^{th} iteration we find

$$\begin{aligned}\mathbf{q}_{(L)} &= \mathbf{U}_{(L,L-1)}\mathbf{q}_{(L-1)} + \mathbf{w}_{(L)} = \\ &= \left(\mathbf{U}_{(L,L-1)}\cdots\mathbf{U}_{(1,0)}\right)\mathbf{q}_{(0)} + \\ &\quad + \left(\mathbf{U}_{(L,L-1)}\cdots\mathbf{U}_{(2,1)}\mathbf{w}_{(1)} + \ldots + \mathbf{U}_{(L,L-1)}\mathbf{w}_{(L-1)} + \mathbf{w}_{(L)}\right) = \\ &= \mathbf{U}_{(L,0)}\mathbf{q}_{(0)} + \mathbf{r}_{(L)}\end{aligned} \tag{46}$$

where $\mathbf{U}_{(L,0)}$ stands for the product-composition (according to the order displayed in equation) of the L matrixes $\mathbf{U}_{(i,i-1)}$. This new matrix represents the transition from $S_{(0)}$ to $S_{(L)}$. The sum between the other round brackets is simply denoted by $\mathbf{r}_{(L)}$.

In the perspective of continuing this procedure, it is now fundamental to notice that

$$\mathbf{U}_{(p,p-1)} = \mathbf{U}_{(hL+p,hL+p-1)}, \quad \forall p, h \in \mathbb{Z} \tag{47}$$

thanks to the periodicity of $\mathbf{\Phi_A}$ and $\mathbf{B}$. Therefore one can obtain

$$\mathbf{U}_{((h+1)L,hL)} = \mathbf{U}_{(L,0)} \equiv \mathbf{U}_g \quad \forall h \in \mathbb{Z} \tag{48}$$

Matrix $\mathbf{U}_g$ is the approximate global monodromy operator representing the dynamic evolution of the system from $S_{(0)}$ to $S_{(L)}$. It will play a central role in the following analysis of stability.

Similarly,

$$\mathbf{w}_{(p+hL)} = \mathbf{w}_{(p)}, \quad \forall p, h \in \mathbb{Z} \tag{49}$$

thanks to the periodicity of $\mathbf{B}_0$. Accordingly,

$$\mathbf{r}_{(hL)} = \mathbf{r}_{(L)} \equiv \mathbf{r}, \quad \forall h \in \mathbb{Z} \tag{50}$$

by also taking into account the periodicity of $\mathbf{U}_{(i,i-1)}$ expressed by Equation (47).

Thus we may write

$$\begin{aligned}\mathbf{q}_{(2L)} &= \mathbf{U}_g\mathbf{q}_{(L)} + \mathbf{r} = \mathbf{U}_g\left(\mathbf{U}_g\mathbf{q}_{(0)} + \mathbf{r}\right) + \mathbf{r} = \\ &= \mathbf{U}_g^2\mathbf{q}_{(0)} + \left(\mathbf{U}_g\mathbf{r} + \mathbf{r}\right)\end{aligned} \tag{51}$$

Again, by iterating

$$\mathbf{q}_{(hL)} = \mathbf{U}_g \mathbf{q}_{((h-1)L)} + \mathbf{r} = \mathbf{U}_g^h \mathbf{q}_{(0)} + \mathbf{R}_h \mathbf{r} \tag{52}$$

where

$$\mathbf{R}_h = \sum_{i=0}^{h-1} \mathbf{U}_g^i \tag{53}$$

is the Neumann series associated to the operator $\mathbf{U}_g$. In order to evaluate system stability, let us determine the asymptotic behaviour of the system by considering the limit $h \to \infty$, as follows

$$\mathbf{q}_{(\infty L)} = \mathbf{U}_g^\infty \mathbf{q}_{(0)} + \mathbf{R}_\infty \mathbf{r} \tag{54}$$

If both the linear operators $\mathbf{U}_g^\infty$ and $\mathbf{R}_\infty$ are bounded in norm, then the final trajectory $\mathbf{q}_{(\infty L)}$ will be bounded for any given history $\mathbf{q}_{(0)}$ and forced vibration term $\mathbf{r}$, hence the system is stable.

This can be achieved by requiring that

$$\left\| \mathbf{U}_g^\infty \mathbf{q}_{(0)} \right\| = 0 \quad \forall \mathbf{q}_{(0)} \in \boldsymbol{\mathcal{C}} \left(S_{(0)} \right) \tag{55}$$

Let us introduce the spectral radius

$$\rho \left(\mathbf{U}_g \right) = \sup \left\{ |\lambda| : \lambda \in \sigma \left(\mathbf{U}_g \right) \right\} \tag{56}$$

where $\sigma(\mathbf{U}_g)$ is the spectrum of the operator $\mathbf{U}_g$. It is possible to demonstrate [39] that the condition (55) is satisfied if and only if

$$\rho \left(\mathbf{U}_g \right) < 1 \tag{57}$$

Moreover, if this condition holds, the sum of the Neumann series $\mathbf{R}_\infty$ does also correspond to a bounded linear operator. In fact, according to operator theory [42], for any continuous linear map $\mathbf{U}_g$

$$\rho \left(\mathbf{U}_g \right) = \lim_{h \to \infty} \left\| \mathbf{U}_g^h \right\|^{\frac{1}{h}} \tag{58}$$

where $\| \cdot \|$ is the chosen operator norm. This is well known as Gelfand's formula. Therefore, given

$$\varepsilon = \frac{1 - \rho}{2} \tag{59}$$

it is possible to find $M \in \mathbb{N}$ such that

$$\left\|\mathbf{U}_g^h\right\|^{\frac{1}{h}} < a = \rho + \varepsilon < 1, \ \forall h > M \quad \Rightarrow \quad \left\|\mathbf{U}_g^h\right\| < a^h, \ \forall h > M \tag{60}$$

Accordingly

$$\left\|\sum_{i=0}^{\infty} \mathbf{U}_g^i\right\| \leq \sum_{i=0}^{\infty} \left\|\mathbf{U}_g^i\right\| \leq \underbrace{\sum_{i=0}^{M} \left\|\mathbf{U}_g^i\right\|}_{<\infty} + \sum_{i=M+1}^{\infty} a^i < \infty, \quad 0 < a < 1 \tag{61}$$

Eventually, for the theorem of total convergence, the Neumann series converges uniformly to a bounded, linear operator $\mathbf{R}_\infty$.

In short, when the spectral radius ρ is smaller than unity, the first term on the right of Equation (54) vanishes, and only the forced vibration contribution $\mathbf{R}_\infty \mathbf{r}$ remains, representing the limit of system trajectory in the intervals $S_{(hL)}$.

This result is very important, because the stability analysis is reduced to the study of the spectral radius, as in the constant speed machining case.

Nevertheless, while in the conventional case with constant spindle speed the final vibrations $\mathbf{q}_{(\infty)}$ (under stable cutting conditions) do only depend on system dynamics (represented by matrix $\mathbf{A}$ and on the external periodic forces (represented by vector $\mathbf{B}_0$), here a subtle and implicit dependence on the regenerative effect (represented by $\mathbf{B}(\varphi)\left(\mathbf{q}\left(\varphi\right) - \mathbf{q}\left(\varphi \Delta \varphi_z\right)\right)$ is still present when $\varphi \to \infty$, which may give rise to vibrational beatings similar to those illustrated in Figure 5e).

Such phenomena could be unacceptable in the perspective of achieving the desired surface finish. Accordingly, new stability criteria based on the analysis of both the spectral radius and the final vibrations could be conceived for a better evaluation of the overall vibration volume characterizing (nominally stable) cutting conditions.

For the sake of illustration, an example of tool tip vibrations in the time and frequency domains is given in Figure 5, by considering a fixed experimental configuration. When performing conventional milling with constant spindle speed, the maximum depth of cut is about 1 mm, while 1.6 mm can be removed by applying the SSV approach, with a theoretical improvement of about 60%. However, as mentioned before the effective applicability of these conditions should be experimentally investigated, since the vibrational

beatings deriving from SSV may cause a poor surface quality. Nevertheless, this is beyond the scope of this paper, and it will be deferred to future research work.

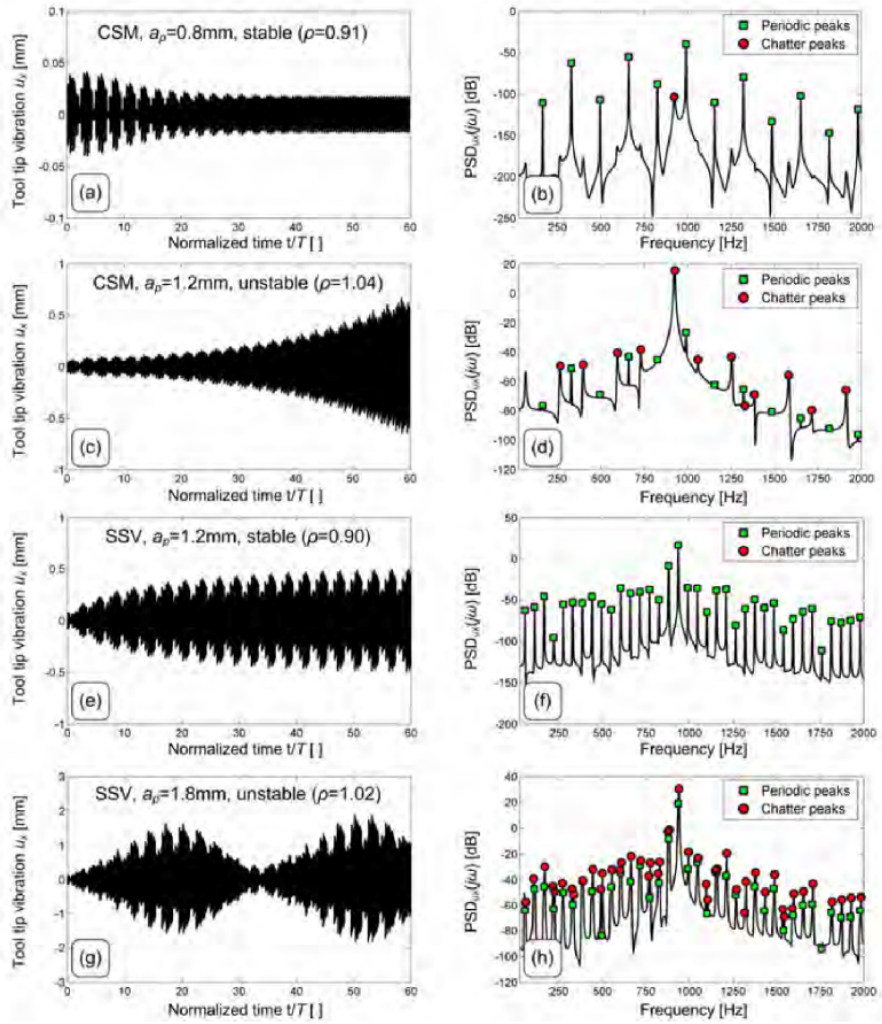

Figure 5: Tool tip vibration in the time and frequency domains, by applying CSM (constant speed machining) and SSV. End-mill cutter with $D = 12.7$ mm, $Z_t = 2$ teeth; down milling with radial immersion $a_L/D = 10\%$; nominal spindle speed $\Omega = 9900$ rpm, nominal feed per tooth $f_z = 0.1$ mm, radial runout $\delta_i = [0.01, -0.01]$ mm; cutting force coefficients $k_{cs} = 600$ MPa, $k_{ns} = 200$ MPa, $k_{cp} = k_{np} = 0$; modal parameters: see Table 3, [31]. SSV parameters: $RVA = 0.3$, $RVF = 1/3$.

5. Algorithms for domain discretization and stability assessment

Basically, both discretization methods compared in this paper approximate the infinite-dimensional monodromy operator $\mathbf{U}_g$ defined in previous section (see Equation (42)) with a finite-dimensional matrix $\hat{\mathbf{U}}_g$. The stability of the system depends on the largest matrix eigenvalue, according to the following stability criterion

$$\max\left\{|\lambda_i| : \lambda_i \in \sigma\left(\hat{\mathbf{U}}_g\right)\right\} \cong \rho < 1 \tag{62}$$

where ρ is the spectral radius and λ_i are the eigenvalues of $\hat{\mathbf{U}}_g$. The main difference between the Semi Discretization Method - SDM - and the Chebyshev Collocation Method - CCM - is the way the monodromy matrix $\hat{\mathbf{U}}_g$ is computed.

5.1. The Semi-Discretization Method - SDM

The Semi Discretization Method [31] can be summarized as follows:

- each (angle) interval $S_{(l)}$ is split into m equally-spaced subintervals $S_{(l,h)}$, defined as

$$S_{(l,h)} = [\varphi_{l,h}, \varphi_{l,h-1}] \tag{63}$$

where

$$\varphi_{l,h} = \varphi_l - h\frac{\Delta\varphi_z}{m}, \qquad h = 0, 1, \ldots, m \tag{64}$$

see Figure (6).

With these assumptions, increasing h implies a decrease of the feed motion angle φ.

- in each subinterval, $\mathbf{A}(\varphi)$, $\mathbf{B}(\varphi)$ and the delayed term $\mathbf{q}(\varphi - \Delta\varphi_z)$ are represented by their zeroth order approximation, as follows

$$\begin{cases} \mathbf{A}(\varphi) \cong \underset{\varphi\in S_{(l,h)}}{\text{mean}}\{\mathbf{A}(\varphi)\} \\ \mathbf{B}(\varphi) \cong \underset{\varphi\in S_{(l,h)}}{\text{mean}}\{\mathbf{B}(\varphi)\} \qquad \text{when } \varphi \in S_{(l,h)} \\ \mathbf{q}(\varphi - \Delta\varphi_z) \cong \frac{1}{2}\left[\mathbf{q}(\varphi_{l-1,h}) + \mathbf{q}(\varphi_{l-1,h-1})\right] \end{cases} \tag{65}$$

By considering the (constant) delayed term as a given input, the original system (35) is reduced to a system of Ordinary Differential Equations - ODEs - within the considered subinterval $S_{(l,h)}$, which can be easily solved by classical techniques;

- by iteratively solving the ODEs corresponding to each subinterval, a monodromy matrix $\hat{\mathbf{U}}_{(l-1,l)}$ can be finally assembled, representing the dynamic transition from $S_{(l-1)}$ to $S_{(l)}$. Specifically, it transforms the column vector

$$\mathbf{v}_{(l-1),\mathrm{SDM}} = \underbrace{\left[\mathbf{q}^{\mathrm{T}}\left(\varphi_{l-1,K,0}\right)\right.}_{\substack{d \text{ initial} \\ \text{conditions for} S_{(l)}}} \underbrace{\left.\mathbf{u}^{\mathrm{T}}\left(\varphi_{l-1,1}\right)\cdots\mathbf{u}^{\mathrm{T}}\left(\varphi_{l-1,m}\right)\right]^{\mathrm{T}}}_{\substack{(2m) \text{ samples of cutter axis position} \\ \text{for Zeroth Order Approximation} \\ \text{of the delayed term}}} \tag{66}$$

  representing the state of the system in $S_{(l-1)}$ into a new vector referring to the following interval $S_{(l)}$. The superscript T denotes vector or matrix transposition, as usual. The dimension of this column vector is

$$\dim\left(\mathbf{v}_{(l-1),\mathrm{SDM}}\right) = d + 2m \tag{67}$$

- the monodromy matrixes $\hat{\mathbf{U}}_{(l,l-1)}$, with l ranging from unity to L, are eventually composed in the correct order to obtain the estimate of the global monodromy matrix $\hat{\mathbf{U}}_g$, i.e.

$$\hat{\mathbf{U}}_g = \hat{\mathbf{U}}_{(L,L-1)}\hat{\mathbf{U}}_{(L-1,L-2)}\cdots\hat{\mathbf{U}}_{(2,1)}\hat{\mathbf{U}}_{(1,0)} \tag{68}$$

  It is fundamental to notice that the dimension (number of rows = number of columns) of the final (square) monodromy matrix is given by Equation (67).

It has to be recalled that the delay expressed in angular coordinates is constant, regardless of the spindle speed modulation. Therefore, it is no longer necessary to approximate the modulated time delay by means of stepwise constant trends, as done by Seguy et al. for adapting the SDM to the SSV case [28].

In section 6, SDM will be applied on the system (35), as well as the new method based on Chebyshev Collocation, in order to allow a strict and fair comparison.

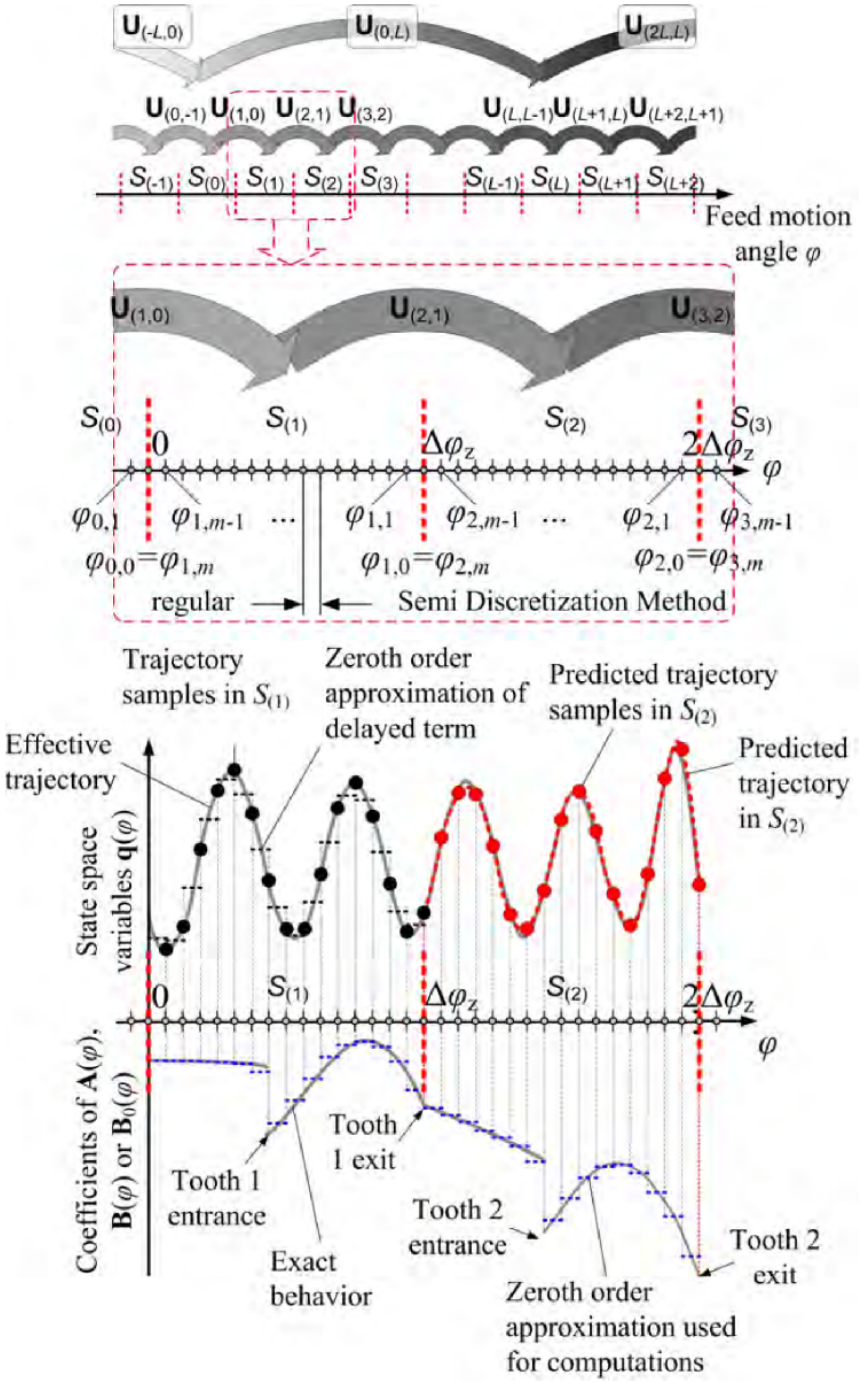

Figure 6: Semi Discretization Method (SDM) concept

5.2. Chebyshev Collocation Method

The new method proposed in this paper is based on the Chebyshev Collocation Method [32][33], which can be summarized as follows:

- each (angle) interval $S_{(l)}$ is split into K subintervals on which $\mathbf{A}(\varphi)$ and $\mathbf{B}(\varphi)$ are of class $\boldsymbol{\mathcal{C}}^1$ (i.e. with continuous first derivative on the whole subinterval), through the points

$$\{(\varphi_{l-1} = \varphi_{l-1,0}),\ \varphi_{l-1,1},\ \varphi_{l-1,2},\ \cdots,\ \varphi_{l-1,K-1},\ (\varphi_{l-1,K} = \varphi_l)\} \tag{69}$$

  located at the kinks (discontinuities) of $\mathbf{A}(\varphi)$ and $\mathbf{B}(\varphi)$ and at the endpoints of interval $S_{(l)}$.

- each subinterval is further split into N uneven subsubintervals according to the Chebyshev Collocation Algorithm, yielding

$$\begin{gathered}\varphi_{l-1,k,i} = \tfrac{1}{2}\left(\varphi_{l-1,k-1} + \varphi_{l-1,k}\right) + \tfrac{1}{2}\cos\left(\tfrac{i\pi}{N}\right)\left(\varphi_{l-1,k} - \varphi_{l-1,k-1}\right) \\ k = 1, \ldots, K; \quad i = 0, 1, \ldots, N\end{gathered} \tag{70}$$

  see Figure (7).

- by applying the spectral methods based on Chebyshev Collocation [43], a monodromy matrix $\hat{\mathbf{U}}_{(l-1,l)}$ is obtained, representing the dynamic transition from $S_{(l-1)}$ to $S_{(l)}$. Specifically, it transforms the column vector

$$\mathbf{v}_{(l-1),\mathrm{CCM}} = \underbrace{\left[\mathbf{u}^{\mathrm{T}}\left(\varphi_{l-1,1,0}\right) \cdots \mathbf{u}^{\mathrm{T}}\left(\varphi_{l-1,1,N}\right) \cdots \mathbf{u}^{\mathrm{T}}\left(\varphi_{l-1,K-1,0}\right) \cdots \mathbf{u}^{\mathrm{T}}\left(\varphi_{l-1,K-1,N}\right)\right.}_{2(N+1)(K-1)\text{ Chebyshev collocation points for polynomial interpolation of the delayed term}}$$
$$\underbrace{\mathbf{q}^{\mathrm{T}}\left(\varphi_{l-1,K,0}\right)}_{\substack{d\text{ initial} \\ \text{conditions for } S_{(l)}}} \underbrace{\left.\mathbf{u}^{\mathrm{T}}\left(\varphi_{l-1,K,1}\right) \cdots \mathbf{u}^{\mathrm{T}}\left(\varphi_{l-1,K,N}\right)\right]^{\mathrm{T}}}_{\substack{2N\text{ Chebyshev collocation points for} \\ \text{polynomial interpolation of the delayed term}}} \tag{71}$$

  representing the state of the system in $S_{(l-1)}$ into a new vector referring to the following interval $S_{(l)}$. The dimension of this column vector is

$$\dim\left(\mathbf{v}_{(l-1),\mathrm{CCM}}\right) = 2K\left(N+1\right) + d - 2 \tag{72}$$

- the monodromy matrixes $\hat{\mathbf{U}}_{(l,l-1)}$, with l ranging from unity to L, are eventually composed in the correct order to obtain the estimate of the global monodromy matrix $\hat{\mathbf{U}}_g$, see Equation (68). Accordingly, the dimension (number of rows = number of columns) of the final monodromy matrix is given by Equation (72).

One main difference with respect to SDM consists in the fact that the coefficients of $\mathbf{A}(\varphi)$, $\mathbf{B}(\varphi)$ and the delayed term $\mathbf{q}(\varphi - \Delta\varphi_z)$ are not considered constant inside each subinterval: they are indeed approximated by interpolating Lagrange polynomials.

Moreover, it should be highlighted that domain discretization performed by Chebyshev Collocation is irregular. Basically, this algorithm takes smaller angle subintervals at the beginning and at the end of each interval $S_{(l)}$ and where discontinuities of the coefficients of $\mathbf{A}(\varphi)$ or $\mathbf{B}(\varphi)$ may be present due to tooth entrance or exit, as shown in Figure 7. The uneven spacing characterizing the Chebyshev Collocation assures a fast convergence of the Lagrange polynomials to the effective curves, when the number of subintervals becomes sufficiently high. The algorithm was developed in the MathWorks MATLAB environment, and it was adapted and improved from the ddec MATLAB suite available on-line at [44].

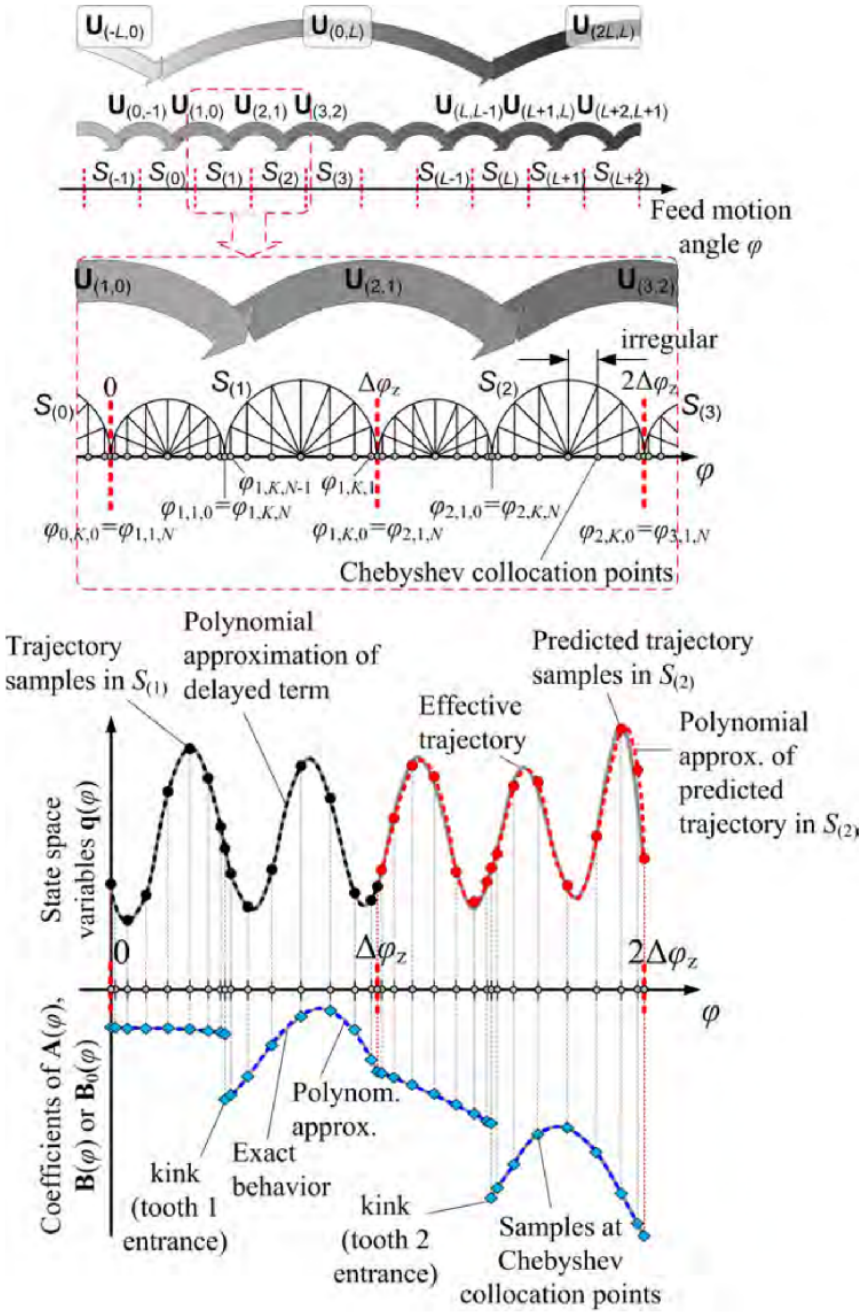

Figure 7: Chebyshev Collocation Method (CCM) concept

6. Evaluation of numerical convergence of the new method and comparison to Semi Discretization Method

It is worth noting that both SDM and CCM discretization algorithms generate the same predictions of system stability, provided that a sufficiently large number of discretization subintervals is chosen for each algorithm. Thus, the methods should be compared in terms of convergence to the theoretical solution and of elaboration time for a desired level of accuracy.

For performing this comparison, a numerical Design of Experiments was carried out. Specifically, several case studies taken from the literature were selected and listed in Table 2.

For each machining system configuration, different cutting configurations were examined, i.e. different relative positions between the tool and the workpiece, such as for instance slotting and peripheral up and down milling. For each cutting configuration, different spindle speed regimes were investigated: Constant Speed Machining (CSM) and SSV machining. Sinusoidal spindle speed modulation was applied by testing different levels of amplitude and frequency modulation coefficients RVA and RVF introduced in Equation (14) and listed in Table 3. For a selected machining system, cutting configuration and spindle speed regime, nine combinations of nominal spindle speed depth of cut were also tested according to the levels outlined in Table 3.

For a given set of machining system parameters, SSV parameters and cutting parameters the spectral radius convergence was finally evaluated.

This was made by first estimating the theoretical spectral radius ρ_{th} by using Chebyshev Collocation Method with a sufficiently high number of collocation points.

Afterwards, spectral radius estimates ρ were computed for an exponentially increasing dimension of the monodromy matrix.

In order to assure a fair comparison between the novel approach and SDM, the spectral radius behaviour was expressed with respect to the monodromy matrix dimension (number of rows = number of columns), which is strictly correlated with memory consumption.

For a given cutting process, the number of state space variables d of the chosen dynamic model and the number of kinks K affecting the matrixes $\mathbf{A}(\varphi)$ and $\mathbf{B}(\varphi)$ are fixed. Therefore, in order to obtain the same dimension of the monodromy matrix, the number of discretization subintervals m considered by SDM and the number of Chebyshev Collocation points N must

Table 2: Experimental cases considered for evaluation of numerical convergence. (m1 = mode 1; m2 = mode 2; NS = not specified; SL = slotting; UP = up milling; DW = down milling.)

	Reference	**[31]**	**[5]**	**[25]**	**[28]**	**[45]**	**[34]**	**New authors' config.**
	Config.	**1**	**2**	**3**	**4**	**5**	**6**	**7**
Modal parameters	G_x [μm/N]	0.747	0.0103	0.0185	0 (∞ stiffness)	0.137(m1), 0.0671(m2)	0.28	0.12
	f_{nx} [Hz]	922	510	426	/	453(m1), 1449(m2)	274	300
	ξ_x []	0.011	0.04	0.03	/	0.123(m1), 0.0165(m2)	0.036	0.055
	G_y [μm/N]	0.747	0.0210	0.211	0.314	0.106(m1), 0.0821(m2)	0.28	0.12
	f_{ny} [Hz]	922	802	384	223	516(m1), 1408(m2)	266	312
	ξ_y []	0.011	0.05	0.02	0.05	0.0243(m1), 0.0324(m2)	0.024	0.121
Tool geometry	**Diameter** D [mm]	12.7	NS	101.6	25	31.75	50	80
	Teeth number Z_t	2	3	8	3	2	5-6	6
Workpiece	**Material**	Al alloy	Al alloy	Al2024	2017A (Al alloy)	Al7075	Ck45	Ck45
	k_{cs} [N/mm^2]	600	900	$\approx$ 600	700	1319	1860	$\approx$ 2000
	k_{ns} [N/mm^2]	200	270	$\approx$ 200	140	788	648	$\approx$ 1000
Cutting parameters	**Range** a_p [mm]	0.1 ÷ 10	10 ÷ 90	0.1÷2.5	0.1 ÷ 6	0.1 ÷ 6	0.1 ÷ 2	0.1 ÷ 2
	Range n [krpm]	5 ÷ 25	5 ÷ 50	0.5÷3.5	1 ÷ 12	1 ÷ 16	0.9÷3.1	0.3÷0.7
Tool-workpiece config.	**Immersion** a_L/D [%]	100 SL; 25 UP; 5 UP; 25 DW; 5 DW.	50 UP; 50 DW.	50 UP; 50 DW.	8 UP; 8 DW.	50 UP; 50 DW.	100 SL; 50 UP; 50 DW.	100 SL; 50 UP; 50 DW.

Table 3: DoE for evaluation of chatter prediction algorithms numerical convergence.

Factor		**Levels**	**Values or range**
Machining system configuration		7	See Table 2
Milling type		3	Slotting (SL), up milling (UP), down milling (DW)
Tool immersion in the workpiece		$2 \div 5$	$5 \div 100$ see Table 2
SSV parameters (sinusoidal perturbation)	RVA	3	0 (CSM), 0.1, 0.3
	RVF	3	0 (CSM), 0.1, 1/3
Cutting parameters	Depth of cut a_p	3	Low, medium and high, given by $(a_{p,min} \cdot (1-h) + h \cdot a_{p,max})$, where $a_{p,min}$ and $a_{p,max}$ are the extremes of the considered depth of cut range and $h = 1/4, 2/4$ and $3/4$ respectively
	Spindle speed n	3	Low, medium and high: minimum, mean and maximum spindle speeds of the range of interest for that configuration, respectively

satisfy the following relation

$$D_{CCM} = \dim\left(\hat{\mathbf{U}}_{g,\mathrm{CCM}}\right) = \dim\left(\hat{\mathbf{U}}_{g,\mathrm{SDM}}\right) = D_{SDM} \tag{73}$$

yielding

$$2K\,(N+1) + d - 2 = 2m + d \tag{74}$$

which can be simplified to

$$K\,(N+1) - 1 = m \approx \frac{D}{2} \tag{75}$$

where D stands for the dimension of the generic monodromy matrix, and the last approximation is valid when the number d of initial conditions is negligible with respect to the total number of subintervals.

In other words, Equation (75) was used for determining the number m of subintervals used by SDM and the number of $(N+1)$ of Chebyshev Collocation points adopted by CCM, for a given monodromy matrix dimension (d and K fixed by the selected machining system and cutting conditions). By so doing, spectral radius convergence rates obtained from the two algorithms could be compared on equal memory consumption conditions.

In order to evaluate spectral radius accuracy, the absolute relative error was computed, as follows

$$\varepsilon_{rel} = \left|\frac{\rho - \rho_{th}}{\rho_{th}}\right| \tag{76}$$

For each algorithm, the minimum monodrmomy matrix dimension D_{min} was determined such that

$$\varepsilon\,(D) < 0.1\% \quad \forall D \geq D_{\mathrm{min}} \tag{77}$$

For each machining system and cutting conditions and for a given monodromy matrix dimension the corresponding spectral radius accuracy was computed and recorded, together with the elaboration time required for assembling the monodromy matrix and for estimating the spectral radius. This time will be called single point elaboration time in the following.

The single point elaboration time T_E corresponding to the minimum matrix dimension for achieving the desired accuracy level D_{min} was identified and recorded.

Eventually, the two algorithms were compared both in terms of memory consumption (D_{min}) and single point elaboration time ($T_E(D_{min})$).

Calculations were performed on a workstation equipped with two 6-core Intel Xeon 3.46 GHz processors and 192 GB of RAM. Up to 12 points were analyzed at the same time using Matlab parallelization in order to reduce the overall computation time. The calculation was no further parallelized at the level of the single point. Single point elaboration time was measured separately, i.e. independently from other computations concurrently running.

In the examples illustrated in Figure 8, it is clear that the spectral radius estimate provided by the new method converged to the theoretical value by requiring a smaller matrix dimension with respect to SDM. In many cases with SSV, SDM did not even reach the required accuracy with a monodromy matrix dimension smaller than 1024. It is worth noting the extremely rapid "exponential" convergence of the new algorithm, whose accuracy was only limited by computer precision.

The new algorithm based on Chebyshev Collocation was much faster than SDM, because it required a smaller monodromy matrix dimension to achieve the desired accuracy and because it was on average faster for a fixed monodromy matrix dimension D. In other words,

$$\left.\begin{array}{l} D_{\mathrm{CCM,min}} < D_{\mathrm{SDM,min}} \\ T_{\mathrm{E,CCM}}\left(D\right) < T_{\mathrm{E,SDM}}\left(D\right) \end{array}\right\} \Rightarrow T_{\mathrm{E,CCM}}\left(D_{\mathrm{CCM,min}}\right) \ll T_{\mathrm{E,SDM}}\left(D_{\mathrm{SDM,min}}\right) \tag{78}$$

For instance, for computing the stability lobes of Figure 1 (based on a grid of 200 spindle speed levels and 100 depth of cut levels) the following total elaboration times were required: 6.7 min for 1a); 33.3 min for 1b); 10 min for 1c) and 126.7 min for 1d). On the other side, SDM would have required from 35 to more than 1342 times longer elaboration times.

The numerical results obtained by performing the whole Design of Experiments are summarized in Figure 9. It can be noticed that about 95% of the investigated points required a smaller monodromy matrix dimension - i.e. less memory consumption - to converge, when Chebyshev Collocation was applied. In addition, 57.8% of the points did not converge when Semi Discretization was applied with a monodromy matrix dimension smaller than 1024, whereas this percentage was only 1.5% with the new algorithm.

Regarding the single point elaboration time, the new algorithm was faster in 99.9% of cases. The geometric average of the ratio between computation times was 199.

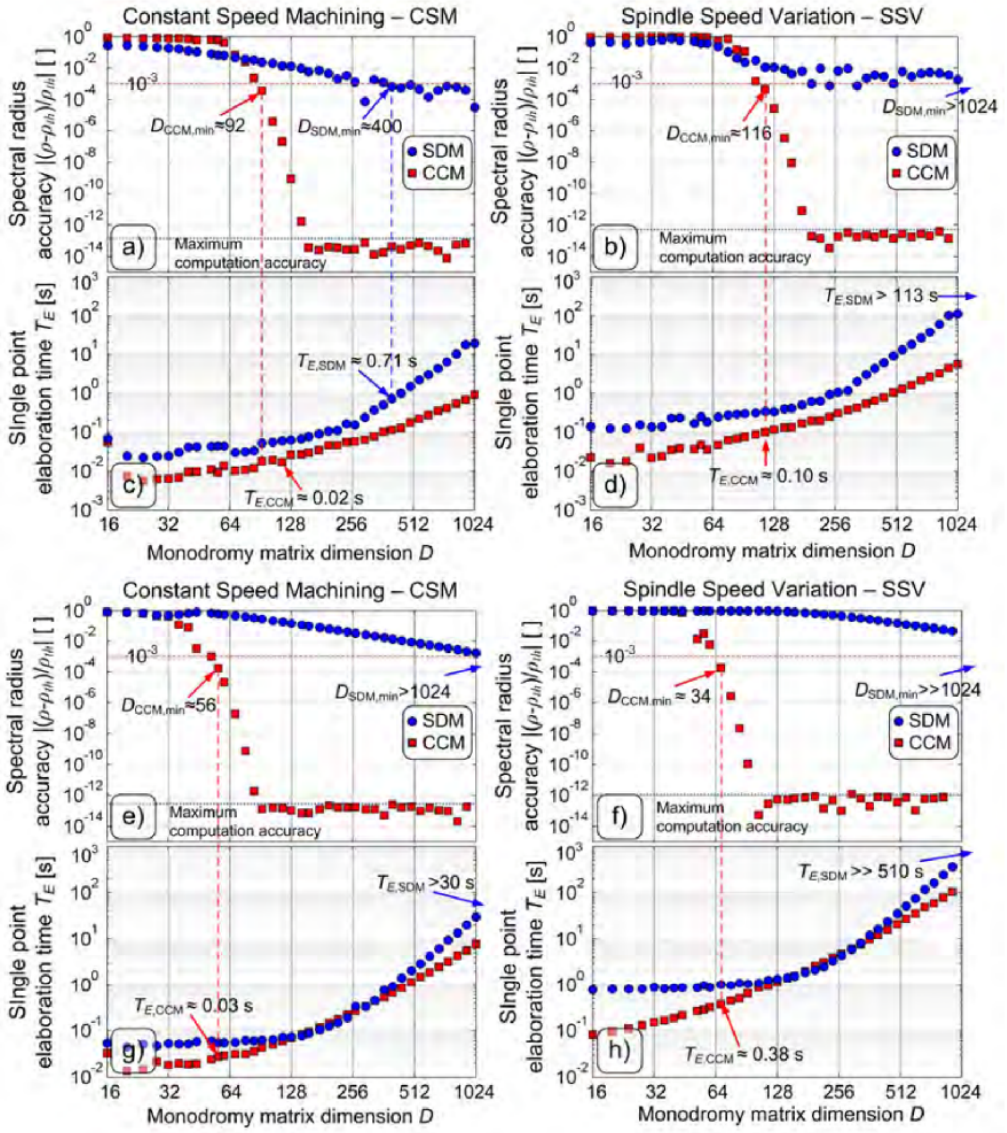

Figure 8: Convergence of chatter prediction algorithms: a), b), c) and d) refer to Insperger configuration [31] (10% down milling, $D = 12.7$ mm, $Z_t = 2$ teeth, aluminum workpiece, $n = 5000$ rpm, $a_p = 1.5$ mm); e), f), g) and h) refer to new authors' configuration (50% down milling, $D = 80$ mm, $Z_t = 6$ teeth, Ck45 workpiece, $n = 300$ rpm, $a_p = 1$ mm). Sinusoidal SSV with $RVA = 0.3$ and $RVF = 1/3$ is applied in b), d), f) and h).

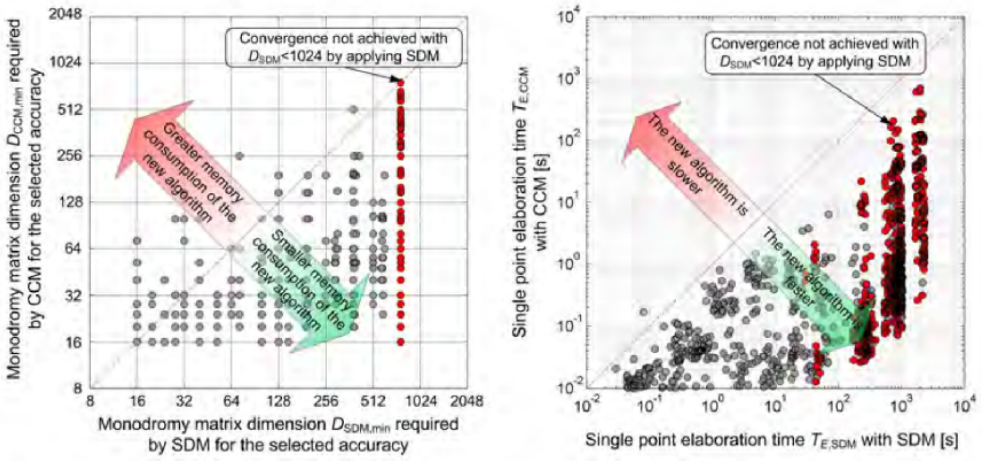

Figure 9: Overall comparison between Chebyshev Collocation and Semi Discretization Method in terms of memory consumption and single point elaboration time, by requiring 99.9% accuracy for spectral radius estimate

From the analysis of the minimum monodromy matrix dimension $D_{CCM,min}$ with respect to different tool-workpiece configurations - see Figure 10 - it was not possible to derive a general rule.

However, SSV generally required a higher monodromy matrix dimension with respect to the simpler case of CSM. As a consequence, the single point elaboration time $T_{E,CCM}$ required by SSV was on average from two to three orders of magnitude greater than that required by the corresponding case with CSM. This fact can be explained by recalling that it is necessary to compute several monodromy matrixes $\hat{\mathbf{U}}_{(l,l-1)}$ for building the global monodromy matrix $\hat{\mathbf{U}}_g$ corresponding to a given milling configuration and cutting condition when SSV is involved, whereas in the case of constant speed machining a single $\hat{\mathbf{U}}_{(l,l-1)}$ is sufficient for achieving the goal.

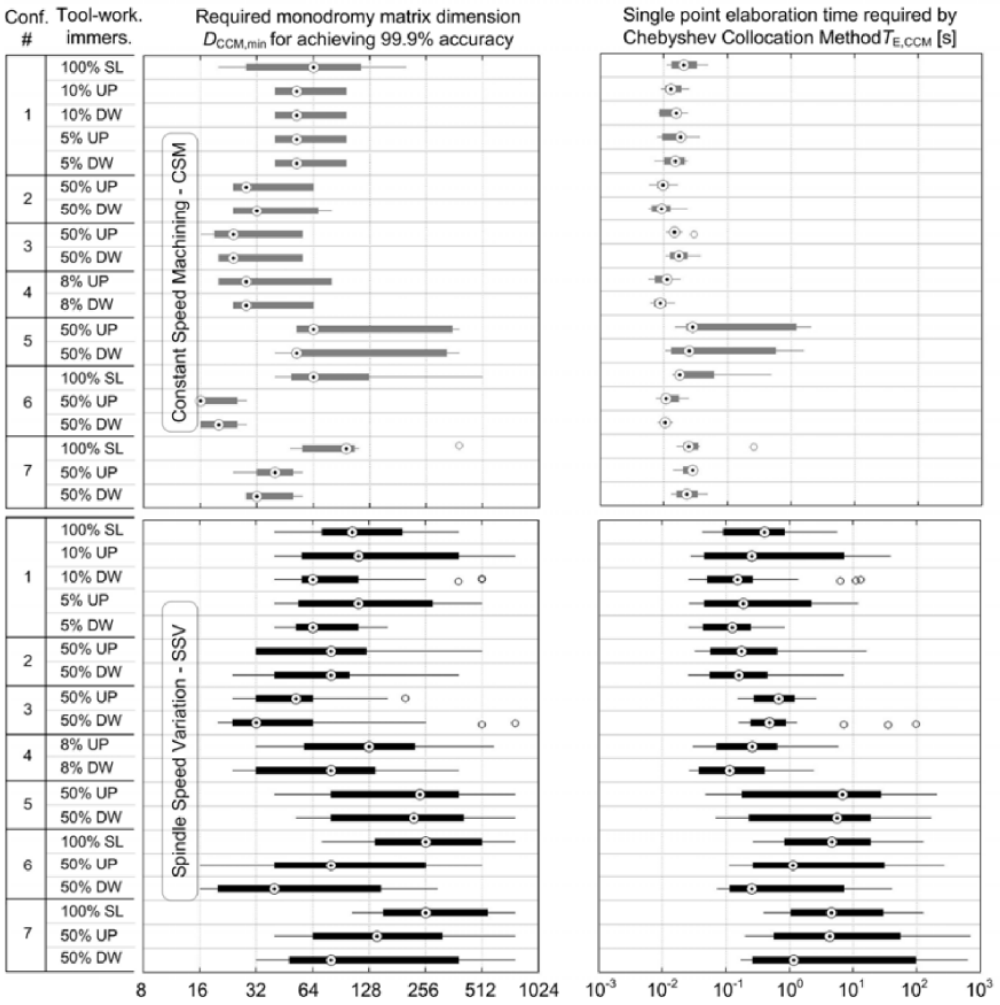

Figure 10: Numerical results in terms of memory consumption and single point elaboration time by applying the new algorithm and by requiring 99.9% accuracy for spectral radius (SL=slotting, UP=up milling, DW=down milling).

Eventually, the detailed comparison between the new algorithm and SDM presented in Figure 11 confirmed the smaller memory consumption of the new algorithm, especially when SSV was applied, except for a few cases mostly referring to CSM. Anyhow, the new algorithm was from about one to three orders of magnitude faster than SDM in all cases, and greatest advantages were on average obtained with SSV.

It was possible to conclude that the new algorithm assured significantly better performances than SDM, allowing an efficient stability evaluation of both CSM and SSV milling operations.

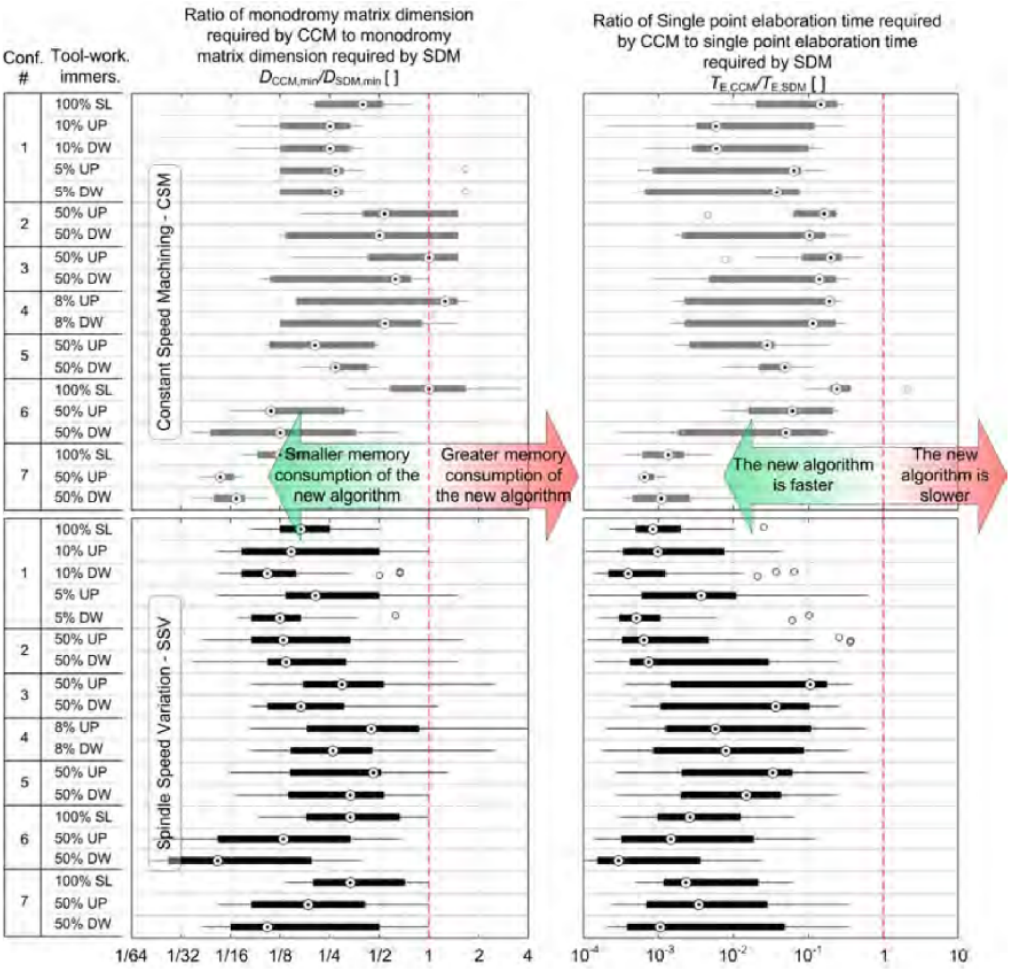

Figure 11: Comparison between the new algorithm based on Chebyshev Collocation Mehtod and SDM, by requiring 99.9% accuracy for spectral radius estimate (SL=slotting, UP=up milling, DW=down milling).

7. Conclusions

A new algorithm for stability evaluation of milling operations with Spindle Speed Variation (SSV) was developed and successfully compared with a state of the art method.

The new method was based on a transformation of coordinates from the time to angular domain, in order to obtain a set of Delay Differential Equations with fixed delay representing the milling process. Afterwards, the core of the method was the application of the Chebyshev Collocation Method for domain discretization and assessment of system stability.

Stability criteria derived from the theory of Delay Differential Equations were extended to milling operations with SSV. It was demonstrated that process stability depends on the spectral radius associated with the obtained monodromy operator representing the dynamic system evolution, as in the case of Constant Speed Machining (CSM). However, it was found out that (nominal stable) forced vibrations may play a crucial role when assessing the overall vibration volume affecting the cutting process, and hence important technological outputs such as the machined surface quality. In this perspective, both the spectral radius and the final forced vibrations can be rapidly estimated by the developed algorithm.

Both the new method and the state of the art method - Semi Discretization Method - considered in this work generated the same predictions of system stability, provided that a sufficiently large number of discretization subintervals or collocation points was chosen for each algorithm. Thus, the methods were compared in terms of convergence to the theoretical solution and of single point elaboration time for a given level of accuracy (99.9%), by assuming the monodromy matrix dimension as main parameter during comparison. For this purpose, several experimental configurations, cutting parameter combinations, as well as different spindle speed regimes (Constant Speed Machining and Spindle Speed Variation) were tested.

When applying the new algorithm, about 95% of the investigated points required less memory consumption to converge. In addition, in 57.8% of cases the Semi Discretization Method did not even converge to the theoretical solution with a monodromy matrix dimension smaller than 1024, whereas this percentage reduced to 1.5% when using the new algorithm.

Regarding the single point elaboration time, the new algorithm was faster in 99.9% of cases. Specifically, it was from one to three orders of magnitude faster than the Semi Discretization Method.

It is worth noting that the greatest advantages both in terms of memory consumption and single point elaboration time were obtained when considering milling operations with Spindle Speed Variation, with respect to conventional milling operations performed at constant spindle speed.

In conclusion, the developed method allows an efficient evaluation of milling process stability both with constant and modulated spindle speed, overcoming the convergence problems which may affect the Semi Discretization Method. Accordingly, the new algorithm is very appealing for industrial applications where computation speed is of primary importance, in the perspective of preventive calibration of SSV parameters and for optimization of the cutting process.

References

[1] I. Grabec, Chaotic dynamics of the cutting process, International Journal of Machine Tools and Manufacture, 28 (1988) 19-32

[2] J. Warminski, G. Litak, M.P. Cartmell, R. Khanin, M. Wiercigroch, Approximate analytical solutions for primary chatter in the non-linear metal cutting model, Journal of Sound and Vibration, 259/4 (2003) 917-933

[3] J. Tlusty, Manufacturing Processes and Equipment, Prentice-Hall, Englewood Cliffs, NJ, (2000)

[4] G. Stepan, Delay-differential equation models for machine tool chatter, Nonlinear Dynamics of Material Processing and Manufacturing, Ed.: F.C. Moon, John Wiley and Sons, New York, (1998), 165-19

[5] Y. Altintas, G. Stepan, D. Merdol, Z. Dombovari, Chatter stability of milling in frequency and discrete time domain, CIRP Journal of Manufacturing Science and Technology, 1 (2008) 35-44

[6] G. Totis, RCPM A new method for robust chatter prediction in milling, International Journal of Machine Tools and Manufacture, 49 (2009) 273-284

[7] M. Sortino, G. Totis, F. Prosperi, Modeling the dynamic properties of conventional and high-damping boring bars, Mechanical Systems and Signal Processing, 34 (2013) 340-352

[8] E. Budak, An Analytical Design Method for Milling Cutters with Non-constant Pitch to Increase Stability, part 2: Application, Journal of Manufacturing Science and Engineering, Trans. ASME, 125 (2003) 35-38

[9] M. Weck, C. Brecher, Werkzeugmaschinen 5: Messtechnische Untersuchung und Beurteilung, dynamische Stabilitt, (2006), Springer-Verlag

[10] F. Yang, B. Zhang, J. Yu, Chatter suppression with multiple time-varying parameters in turning, Journal of Materials Processing Technology, 141 (2003) 431-438

[11] D. Mei, T. Konga, A.J. Shihb, Z. Chen, Magnetorheological fluid-controlled boring bar for chatter suppression, J. Mater. Process. Technol., 209 (2009) 1861-1870.

[12] J.L. Dohner, J.P. Lauffer, T.D. Hinnerichs, N. Shankar, M. Regelbrugge, C.M. Kwan, R. Xu, B. Winterb, Mitigation of Chatter Instabilities by Active Structural Control, Journal of Sound and Vibration, 269 (2004) 197-211

[13] C. Brecher, D. Manoharan, U. Ladra, H.-G. Kpken, Chatter suppression with an active workpiece holder, Prod. Eng. Res. Devel., 4 (2010) 239-245

[14] N.J.M. van Dijk, E.J.J. Doppenberg, R.P.H. Faassen, N. van de Wouw, J.A.J. Oosterling, H. Nijmeijer, Automatic in-process chatter avoidance in the high speed milling process, ASME Journal of Dynamic Systems, Measurement and Control, 132 (2010)

[15] T. Stoferle, H. Grab, Vermeiden von Ratterschwingungen durch periodische Drehzahlanderung, Werkstatt und Betrieb, 105 (1972) 727.

[16] J.S. Sexton, B.J. Stone, The stability of machining with continuously varying spindle speed, Annals of the CIRP, 27 (1978) 321-326.

[17] T.C. Tsao, M.W: McCarthy, S.G. Kapoor, A new approach to stability analysis of variable speed machining systems, International Journal of Machine Tools and Manufacture, 33/6 (1993) 791-808

[18] P. Albertelli, S. Musletti, M. Leonesio, G. Bianchi, M. Monno, Effectiveness and feasibility of spindle speed variation in turning, Proceedings of the 10th AITeM Conference, Neaples, Italy, (2011)

[19] M.X. Zhao, B. Balachandran, Dynamics and stability of milling process, International Journal of Solid and Structures, 38 (2001) 2233-2248

[20] M.L. Campomanes, Y. Altintas, An Improved Time Domain Simulation for Dynamic Milling at Small Radial Immersions, Trans. ASME, Manufacturing and Engineering and Science, 125 (2003) 29-38

[21] T. Insperger, T. L. Schmitz, T. J. Burns, G. Stepan, Comparison of analytical and numerical simulations for variable spindle speed turning, Proceedings of IMECE03: 2003 ASME International Mechanical Engineering Congress, Washington, USA

[22] M. Zatarain, I. Bediaga, J. Munoa, R. Lizarralde, Stability of milling processes with continuous spindle speed variation: Analysis in the frequency and time domains, and experimental correlation, CIRP Annals - Manufacturing Technology, 57 (2008) 379-384

[23] E. Al-Regib, J. Ni, S.-H. Lee, Programming spindle speed variation for machine tool chatter suppression, International Journal of Machine Tools and Manufacture, 43 (2003) 1229-1240

[24] S. Jayaram, S. G. Kapoor, R. E. DeVor, Analytical Stability Analysis of Variable Spindle Speed Machining, ASME Journal of Manufacturing Science and Engineering, 122 (2000) 391-397

[25] S. Sastry, S. G. Kapoor, R. E. DeVor, Floquet Theory Based Approach for Stability Analysis of the Variable Speed Face-Milling Process, ASME Journal of Manufacturing Science and Engineering, 124 (2002) 10-17

[26] A. Yilmaz, E. Al-Regib, J. Ni, Machine Tool Chatter Suppression by Multi-Level Random Spindle Speed Variation, ASME Journal of Manufacturing Science and Engineering, 124 (2002) 208-216

[27] T. Insperger, G. Stepan, Stability analysis of turning with periodic spindle speed modulation via semidiscretization, Journal of Vibration and Control, 10 (2004) 1835-1855

[28] S. Seguy, T. Insperger, L. Arnaud, G. Dessein, G. Peign, On the stability of high-speed milling with spindle speed variation, Int. J. Adv. Manuf. Technol., 48 (2010) 883-895

[29] X. Long, B. Balachandran, Stability of Up-milling and Down-milling Operations with Variable Spindle Speed, Journal of Vibration and Control, 16(7-8) (2010) 1151-1168

[30] Y. Altintas, E. Budak, Analytical Prediction of Stability Lobes in Milling, Annals of the CIRP, 44 (1995) 357-362.

[31] T. Insperger, G. Stpn, Updated semi-discretization method for periodic delay-differential equations with discrete delay, International Journal for Numerical Methods in Engineering, 61 (2004) 117-141.

[32] E. Bueler, Chebyshev Collocation for Linear, Periodic, Ordinary and Delay Differential Equations: a Posteriori Estimates, (2004), Cornell University Library, http://arxiv.org/, math.NA/0409464

[33] E.A. Butcher, P. Nindujarla, E. Bueler, Stability of Up- and Down-Milling using Chebyshev Collocation Method, Proceedings of ASME 2005 International Design Engineering Technical Conferences and Computers and Information in Engineering Conference IDETC/CIE 2005, California, USA

[34] E. Kuljanic, M. Sortino, G. Totis, Quick Chatter Prediction Method - QCPM, an Innovative Algorithm for Chatter Prediction in Milling, 8th AITeM Conference, (2007), Montecatini Terme, Italy

[35] G. Genta, Dynamics of Rotating Systems, (2005), Springer

[36] J. Gradisek, M. Kalveram, T. Insperger, K. Weinert, G. Stepan, E. Govekar, I. Grabec, On stability prediction for milling, International Journal of Machine Tools and Manufacture, 45 (2005) 768-781

[37] Y. Altintas, M. Weck, Chatter stability of metal cutting and grinding, Annals of the CIRP, 53/2 (2004) 619-642

[38] Y. Altintas, Manufacturing automation: Metal Cutting Mechanics, Machine Tool Vibrations, and CNC Design, (2000),Cambridge University Press

[39] G. Totis, Research on the Dynamics of Milling, PhD Dissertation, 2008, University of Udine

[40] M. Pakdemirli, A.G. Ulsoy, Perturbation Analysis of Spindle Speed Variation in Machine Tool Chatter, Journal of Vibration and Control, 3 (1997) 261-278

[41] E. Bueler, E. Butcher, Stability of periodic linear delay-differential equations and the Chebyshev approximation of fundamental solutions, UAF Dept. of Mathematical Sciences Technical Report 2002-2003

[42] V. Hutson, J.S. Pym, Applications of Functional Analysis and Operator Theory, (1980), Academic Press, New York

[43] L.N. Trefethen, Spectral Methods in MATLAB, (2000), SIAM Press, Philadelphia

[44] http://www.cs.uaf.edu/

[45] Y. Altintas, S. Engin, Generalized Modeling of Mechanics and Dynamics of Milling Cutters, Annals of the CIRP, 50/1 (2001) 25-30